

Band representation, band connectivity and atomic limit

Jing Zhang

*Department of Physics and Institute of Advanced Studies,
Tsinghua University, Beijing 100084, PRC and Blackett Laboratory,
Department of Physics, Imperial College London,
Prince Consort Road, London SW7 2AZ, UK*

(Dated: October 1, 2021)

Abstract

The “band representation”, formulated by Zak in the 80’s, is widely used in recent studies of topological phase of material. However, either the basis of band representation contains an error in its definition or the transformation properties employed is missing phase terms. This manuscript present a clear definition of the basis and an alternative derivation of analytical transformation properties of the band representation. It identifies explicitly what occurs at high symmetry point on the surface of Brillouin zone and allows decomposition of band representation into irreducible representations of the space group anywhere in the representation domain of the Brillouin zone. Two different Fourier transform conventions in defining the band representation induced from the same localised Wannier functions are discussed and identified as related by a simple gauge transformation. The tight binding band representation are used as basis in deriving the tight binding Hamiltonian using group theoretical technique. With the analytical tools afforded by the representation matrices of the band representations, a clear methodology is developed to obtain band connectivity in the representation domain and establish which does not have an atomic limit. Elementary band representations is shown to be fully connected in the atomic limit. In particular, the band representation induced from spin-ful p_z orbital on Wyckoff position 2c of honeycomb lattice has a connectivity with atomic limit and the topological nature of the band in graphene can arises from such connection and spin orbit interaction induced gap at K point. Combined with symmetry compliant tight binding Hamiltonian, one can examine the homeomorphic transformation of bands induced by changes in the parameters in the model and establish if band inversion has occurred.

I. INTRODUCTION

Band representation(BR), originally formulated by Zak^{1,2}, is receiving attention due to its application in studies of topology in the electronic band structure in wave-vector space³⁻⁹. The original work was extended by Evarestov and Smirnov¹⁰ and used in the tabulation of band representation (BANDREP) in the Bilbo Crystallgraphic Server¹¹. Much of the topological quantum chemistry work is dubbed as the study of band structure without the Hamiltonian. There is an extensive description of group theoretical approach in condensed matter physics, including BR¹². Central to its application is the band connectivity (continuity chords) between high symmetry points (HSP) in the Representation Domain(RD) of the first Brillouin Zone(BZ). The coincidence of band connectivity is one of the necessary conditions for equivalence between any two BRs. There are existing analysis of band connectivity^{3,9,10,13} but the work is largely restricted to decomposition of BR at HSPs and graph analysis. A more theoretical work on band connectivity was carried out by Barcy¹⁴. There is an absence of clear methodology of analysing band connectivity in the atomic limit. The transformation rules derived in the literature exhibit a significant error in phase and does not identify what occurs at HSPs on the surface of BZ¹⁵. Intuitively, one expect the representation matrices to be dependent on the Wyckoff position, the wave-vector \mathbf{k} but not the lattice translation associated with the site symmetry group.

The band representations are infinite dimensional representation of the space group. This is realised in real space through Wannier functions localised on the crystallographic orbit of Wyckoff position or its Fourier transform in wave-vector space with each allowed wave-vector in the Brillouin zone. In defining the band representations in k-space, there are two conventions which lead to the tight binding (TB) basis and the Zak basis. The original Slater-Koster formulation¹⁶ of the tight binding theory is based on the TB basis whereas the recent analysis of band topology are based on the Zak band representation. In the study of band topology, the concept of ‘Elementary Band Representation(EBR)’¹⁷, ‘Composite Band Representation (CBR)’ and ‘Physical Elementary Band Representation(PEBR)’¹⁸ were introduced³. There had been claims¹⁹ and counter claims^{20,21} of full connectivity of EBR. These may be due to a lack of transparent methodology to establish band connectivity and finding what is in the atomic limit. The equivalence between any two band representations requires that the decomposition of the two band representations in-terms of irreducible representations

(irrep) of space group \mathcal{G} to be the same at all the points within the BZ. This is a necessary condition and the identification of equivalence between two band representations are cumbersome. To examine topological phase transitions under symmetry compliant deformation of the Hamiltonian, it is also desirable to have a symmetry compliant TB model which include all symmetry permitted interactions. Such model can be used in an analogous way to the Su-Schrieffer-Heager model for poly-acetylene for clarification of topological order. In this manuscript, the transformation laws of the TB & Zak basis are derived explicitly (section II) for a general space group (\mathcal{G}). A tight binding Hamiltonian is constructed using group theoretical method utilising the TB basis (section III). The analytical form of the representation matrices of band representation allows construction and use of group theoretical tools such as projection operators. In section IV, decomposition of BR into irrep of \mathcal{G} is first derived using Frobenius reciprocity theorem, working towards band connectivity. In section V, projection operators are developed to establish links between nodes of EBR at different HSPs under atomic limit and classify them as simple or complex type depending on number of nodes involved. Two nodes (unitary irreps at a given $\kappa \in \text{RD}$) are linked if the product of projection operator at these notes are non-zero in either order. The decomposition of complex links into simple link in physical band connectivity establish the band connectivity of EBR. This goes beyond what can be established using compatibility relations and graph theory⁹. The EBR under atomic limit is shown to be fully connected. In particular, the EBR induced from spin-ful p_z orbital on Wyckoff position 2c (space group 191) is shown to have connectivity which is connected in the atomic limit. The connectivity can not be removed by inter-site spin orbit interaction induced gap or inverting the band symmetry at Γ^{20} . Utilising the symmetry compliant TB model, concepts of dynamic (with interaction) equivalence of BRs and band inversion are discussed in relation to band connectivity in the atomic limit.

II. BAND REPRESENTATION OF SPACE GROUP

Given a Wyckoff position τ_α , the action¹⁹ of all elements of space group \mathcal{G} generates the crystallographic orbit of the Wyckoff position. Thus all the Wannier functions centred on these orbit given by $\mathbf{t}_\ell + \tau_\alpha$ form an invariant space under \mathcal{G} , or an infinite dimensional representation of \mathcal{G} . A typical Wannier function has the form $\phi_{\mu,i}^{\tau_\alpha}(\mathbf{r} - (\mathbf{t}_\ell + \tau_\alpha))$ whose

localisation centre is defined by $(\mathbf{t}_\ell + \boldsymbol{\tau}_\alpha)$. The motivation for the construction of band representation in wave-vector space is clear. Instead of expressing any wave function as linear combination of Wannier functions located over the crystallographic orbit of the Wyckoff position, a Fourier transform is performed in recognition of the variable $\mathbf{t}_\ell + \boldsymbol{\tau}_\alpha$ having the translational symmetry of the lattice. This transforms the infinite dimensional representation in terms of the Wannier functions to direct sums of finite dimensional representation at each of the infinite number of allowed wave vector \mathbf{k} labelled by \mathbf{k} , $\boldsymbol{\tau}_\alpha$, μ , and i . The basis at different \mathbf{k} 's are orthogonal to each other. Different atoms (located on different Wyckoff positions) are referred to by the label $\boldsymbol{\tau}_\alpha$ and different orbitals are partitioned into irrep μ of the site symmetry group G^τ . The basis of band representation is explicitly dependent on the Wyckoff position¹⁵ and have the following Fourier transform in its definition

$$\Psi_{\boldsymbol{\tau}_\alpha, \mu, i}^{\mathbf{k}}(\mathbf{r}) = \langle \mathbf{r} | \mathbf{k}, \boldsymbol{\tau}_\alpha, \mu, i \rangle_{\text{Zak}} = \Omega^{-1} \sum_{\ell} \exp\{i\mathbf{k} \cdot \mathbf{t}_\ell\} \phi_{\mu, i}^{\boldsymbol{\tau}_\alpha}(\mathbf{r} - (\mathbf{t}_\ell + \boldsymbol{\tau}_\alpha)) \quad (1)$$

where the summation is over the lattice vector \mathbf{t}_ℓ indexed by ℓ and $\phi_{\mu, i}^{\boldsymbol{\tau}_\alpha}(\mathbf{r} - (\mathbf{t}_\ell + \boldsymbol{\tau}_\alpha))$ is the Wannier function transforming according to irrep μ of the site-symmetry group and localised at $\mathbf{t}_\ell + \boldsymbol{\tau}_\alpha$. The convention

$$\Psi_{\boldsymbol{\tau}_\alpha, \mu, i}^{\mathbf{k}} = \Psi_{\boldsymbol{\tau}_\alpha, \mu, i}^{\mathbf{k} + \mathbf{K}}, \quad (2)$$

where \mathbf{K} is a reciprocal lattice vector, can be easily established under this definition of the Fourier transform, a property not generally expected from Bloch functions. This is referred to as the Zak basis in this manuscript though modification is made to the original definition.

The alternative, or more conventional Fourier transform, in the band representation of \mathcal{G} induced from a Wannier function $\phi_{\mu, i}^{\boldsymbol{\tau}_\alpha}$ is given in the Bloch sum:

$$\psi_{\boldsymbol{\tau}_\alpha, \mu, i}^{\mathbf{k}}(\mathbf{r}) = \langle \mathbf{r} | \mathbf{k}, \boldsymbol{\tau}_\alpha, \mu, i \rangle_{\text{TB}} = \Omega^{-1} \sum_{\ell} \exp\{i\mathbf{k} \cdot (\mathbf{t}_\ell + \boldsymbol{\tau}_\alpha)\} \phi_{\mu, i}^{\boldsymbol{\tau}_\alpha}(\mathbf{r} - (\mathbf{t}_\ell + \boldsymbol{\tau}_\alpha)) \quad (3)$$

This is the normal basis from which the Slater-Koster formulation of tight binding model¹⁶ is constructed. It is referred to as the TB basis of band representation, or simply the TB basis in this manuscript. The Zak and TB basis for band representation differs by a \mathbf{k} dependent gauge transformation:

$$\psi_{\boldsymbol{\tau}_\alpha, \mu, i}^{\mathbf{k}} = \exp(i\mathbf{k} \cdot \boldsymbol{\tau}_\alpha) \Psi_{\boldsymbol{\tau}_\alpha, \mu, i}^{\mathbf{k}} \quad (4)$$

Thus the Hamiltonian in these two bases are simply related to each other by the unitary gauge transformation described in Eq.(4). Whilst the Zak basis clearly has desirable properties of Eq.(2) in the wave-vector space, we shall see that it is much easier to write down

transformation under space group operations for the TB basis and construct symmetry permitted Hamiltonian by method of invariant. The general validity of the TB model indicate the modification of the original definition of Zak basis is necessary.

When decomposition of band representation into irreducible form at a given wave-vector is performed, it is necessary to have the band representation processing the same gauge condition in \mathbf{k} space as the irreducible representations of \mathcal{G}^k . The irreducible representations of \mathcal{G}^k are normally chosen to follow Eq.(2)²². It is necessary to utilise the Zak basis when considering decomposition of band representations and discussing topological properties of the BR. Fortunately, the transformation properties of Zak basis can be easily obtained from that of the TB basis with the aide of Eq.(4). As we shall see, it is also advantage to adjust the conventions on irreducible representation of little group of \mathbf{k} to ensure they share the same factoring system as the Zak basis where a projective representations exist on high symmetry points (HSP) on the surface of Brillouin zone for non-symmorphic space groups.

Let's consider the action of a general space group element $\{R|\mathbf{v} + \mathbf{t}\}$ (here \mathbf{v} is the non-lattice translation associated with R) acting on the basis function in Eq.(3). With active interpretation, the action of a symmetry operation $g \in \mathcal{G}$ on a function of position $\psi(\mathbf{r})$ yield the numerical relation $g \bullet \psi(\mathbf{r}) = \psi(g^{-1}\mathbf{r})$. Hence

$$\begin{aligned} \left\langle \mathbf{r} \mid \hat{S}(\{R|\mathbf{v} + \mathbf{t}\}) \mid \mathbf{k}, \boldsymbol{\tau}_\beta, \mu, i \right\rangle_{\text{TB}} &= \hat{S}(\{R|\mathbf{v} + \mathbf{t}\}) \psi_{\boldsymbol{\tau}_\beta, \mu, i}^k(\mathbf{r}) \\ &= \psi_{\boldsymbol{\tau}_\beta, \mu, i}^k(\{R^{-1}| - R^{-1}(\mathbf{v} + \mathbf{t})\} \mathbf{r}) = \psi_{\boldsymbol{\tau}_\beta, \mu, i}^k(R^{-1}\mathbf{r} - R^{-1}(\mathbf{v} + \mathbf{t})) \\ &= \Omega^{-1} \sum_{\ell} \exp\{i\mathbf{k} \cdot (\mathbf{t}_\ell + \boldsymbol{\tau}_\beta)\} \phi_{\boldsymbol{\tau}_\beta}^{\mu, i}(R^{-1}\mathbf{r} - R^{-1}(\mathbf{v} + \mathbf{t}) - (\mathbf{t}_\ell + \boldsymbol{\tau}_\beta)) \\ &= \Omega^{-1} \sum_{\ell} \exp\{i\mathbf{k} \cdot (\mathbf{t}_\ell + \boldsymbol{\tau}_\beta)\} \phi_{\mu, i}^{\boldsymbol{\tau}_\beta}(R^{-1}[\mathbf{r} - \{R|\mathbf{v} + \mathbf{t}\}(\mathbf{t}_\ell + \boldsymbol{\tau}_\beta)]) \end{aligned}$$

Since $\{R|\mathbf{v} + \mathbf{t}\}$ is an element of the space group, hence

$$\begin{aligned} \{R|\mathbf{v} + \mathbf{t}\}(\mathbf{t}_\ell + \boldsymbol{\tau}_\beta) &= \mathbf{t}'_\ell + \boldsymbol{\tau}_\alpha, \\ \mathbf{t}_\ell + \boldsymbol{\tau}_\beta &= \{R^{-1}| - R^{-1}(\mathbf{v} + \mathbf{t})\}(\mathbf{t}'_\ell + \boldsymbol{\tau}_\alpha), \end{aligned}$$

where $\boldsymbol{\tau}_\alpha$ may point to the same or equivalent Wyckoff position modulo primitive cell. The summation over all \mathbf{t}_ℓ is the same as over all \mathbf{t}'_ℓ . Therefore

$$\begin{aligned} \hat{S}(\{R|\mathbf{v} + \mathbf{t}\}) \psi_{\boldsymbol{\tau}_\beta, \mu, i}^k(\mathbf{r}) &= \Omega^{-1} \sum_{\ell} \exp\{i\mathbf{k} \cdot \{R^{-1}| - R^{-1}(\mathbf{v} + \mathbf{t})\}(\mathbf{t}'_\ell + \boldsymbol{\tau}_\alpha)\} \phi_{\mu, i}^{\boldsymbol{\tau}_\beta}(R^{-1}[\mathbf{r} - (\mathbf{t}'_\ell + \boldsymbol{\tau}_\alpha)]) \\ &= \Omega^{-1} \exp\{-iR\mathbf{k} \cdot (\mathbf{v} + \mathbf{t})\} \sum_{\ell} \exp\{iR\mathbf{k} \cdot (\mathbf{t}'_\ell + \boldsymbol{\tau}_\alpha)\} \phi_{\mu, i}^{\boldsymbol{\tau}_\beta}(R^{-1}[\mathbf{r} - (\mathbf{t}'_\ell + \boldsymbol{\tau}_\alpha)]) \end{aligned}$$

Let $\mathbf{u} = \mathbf{r} - (\mathbf{t}'_\ell + \boldsymbol{\tau}_\alpha)$, we obtain

$$\begin{aligned}\hat{S}(\{R|\mathbf{v} + \mathbf{t}\})\psi_{\boldsymbol{\tau}_\beta, \mu, i}^{\mathbf{k}}(\mathbf{r}) &= \Omega^{-1} \exp\{-iR\mathbf{k} \cdot (\mathbf{v} + \mathbf{t})\} \sum_\ell \exp\{iR\mathbf{k} \cdot (\mathbf{t}'_\ell + \boldsymbol{\tau}_\alpha)\} \phi_{\mu, i}^{\boldsymbol{\tau}_\beta}(R^{-1}\mathbf{u}) \\ &= \Omega^{-1} \exp\{-iR\mathbf{k} \cdot (\mathbf{v} + \mathbf{t})\} \sum_\ell \exp\{iR\mathbf{k} \cdot (\mathbf{t}'_\ell + \boldsymbol{\tau}_\alpha)\} \hat{U}(R) \phi_{\mu, i}^{\boldsymbol{\tau}_\beta}(\mathbf{u})\end{aligned}$$

Here the operator $\hat{U}(R)$ does not involve translation and acts on the local orbital centred at the Wyckoff position $\mathbf{t}'_\ell + \boldsymbol{\tau}_\alpha$ with vector \mathbf{u} as its parameter. However, the action of $\hat{U}(R)$ on $\phi_{\mu, i}^{\boldsymbol{\tau}_\beta}(\mathbf{u})$ is not defined when $\boldsymbol{\tau}_\alpha \neq \boldsymbol{\tau}_\beta$ or $R \notin \tilde{G}_\beta^\tau$. To overcome this, we decompose $R = R_\alpha^\tau \cdot R_{\leftarrow}^\tau(R, R_\alpha^\tau) \cdot R_\beta^{\tau-1}$ as in Eq.(A7) and define the following:

$$\hat{U}(R_\alpha^\tau) \phi_{\mu, i}^{\boldsymbol{\tau}_1}(\mathbf{u}) = \phi_{\mu, i}^{\boldsymbol{\tau}_\alpha}(\mathbf{u}).$$

This implies

$$\begin{aligned}\hat{U}(R_\beta^{\tau-1}) \phi_{\mu, i}^{\boldsymbol{\tau}_\beta}(\mathbf{u}) &= \phi_{\mu, i}^{\boldsymbol{\tau}_1}(\mathbf{u}), \\ \hat{U}(R_{\leftarrow}^\tau(R, R_\alpha^\tau) \cdot R_\beta^{\tau-1}) \phi_{\mu, i}^{\boldsymbol{\tau}_\beta}(\mathbf{u}) &= \sum_j D^\mu(R_{\leftarrow}^\tau(R, R_\alpha^\tau))_{ji} \phi_{\mu, j}^{\boldsymbol{\tau}_1}(\mathbf{u}), \\ \hat{U}(R_\alpha^\tau \cdot R_{\leftarrow}^\tau(R, R_\alpha^\tau) \cdot R_\beta^{\tau-1}) \phi_{\mu, i}^{\boldsymbol{\tau}_\beta}(\mathbf{u}) &= \sum_j D^\mu(R_{\leftarrow}^\tau(R, R_\alpha^\tau))_{ji} \phi_{\mu, j}^{\boldsymbol{\tau}_\alpha}(\mathbf{u}).\end{aligned}\quad (5)$$

The definition of $\phi_{\mu, i}^{\boldsymbol{\tau}_\alpha}(\mathbf{u})$ can be thought of as placing such orbital on the equivalent Wyckoff position $\mathbf{t}'_\ell + \boldsymbol{\tau}_\alpha$ and constructing the associated Bloch sum. Restoring \mathbf{u} in terms of \mathbf{r} , the action of $\{R|\mathbf{v} + \mathbf{t}\}$ yield

$$\begin{aligned}\hat{S}(\{R|\mathbf{v} + \mathbf{t}\})\psi_{\boldsymbol{\tau}_\beta, \mu, i}^{\mathbf{k}}(\mathbf{r}) &= \Omega^{-1} \exp\{-iR\mathbf{k} \cdot (\mathbf{v} + \mathbf{t})\} \sum_\ell \exp\{iR\mathbf{k} \cdot (\mathbf{t}'_\ell + \boldsymbol{\tau}_\alpha)\} \times \\ &\quad \sum_j D^\mu(R_{\leftarrow}^\tau(R, R_\alpha^\tau))_{ji} \phi_{\mu, j}^{\boldsymbol{\tau}_\alpha}(\mathbf{r} - (\mathbf{t}'_\ell + \boldsymbol{\tau}_\alpha)) \\ &= \Omega^{-1} \exp\{-iR\mathbf{k} \cdot (\mathbf{v} + \mathbf{t})\} \sum_j D^\mu(R_{\leftarrow}^\tau(R, R_\alpha^\tau))_{ji} \times \\ &\quad \sum_\ell \exp\{iR\mathbf{k} \cdot (\mathbf{t}'_\ell + \boldsymbol{\tau}_\alpha)\} \phi_{\mu, j}^{\boldsymbol{\tau}_\alpha}(\mathbf{r} - (\mathbf{t}'_\ell + \boldsymbol{\tau}_\alpha)) \\ &= \exp\{-iR\mathbf{k} \cdot (\mathbf{v} + \mathbf{t})\} \sum_j D^\mu(R_{\leftarrow}^\tau(R, R_\alpha^\tau))_{ji} \psi_{\boldsymbol{\tau}_\alpha, \mu, j}^{R\mathbf{k}}(\mathbf{r}).\end{aligned}\quad (6)$$

where $R = R_\alpha^\tau \cdot R_{\leftarrow}^\tau(R, R_\alpha^\tau) \cdot R_\beta^{\tau-1}$ and $\{R|\mathbf{v} + \mathbf{t}\}(\mathbf{t}_\ell + \boldsymbol{\tau}_\beta) = \mathbf{t}'_\ell + \boldsymbol{\tau}_\alpha$. Eq.(6) is a functional relation as both side of the equation are functions of \mathbf{r} .

It is clear that

$$\hat{S}(\{E|\mathbf{t}\})\psi_{\tau_\beta,\mu,i}^{\mathbf{k}}(\mathbf{r}) = \exp\{-i\mathbf{k} \cdot \mathbf{t}\}\psi_{\tau_\beta,\mu,i}^{\mathbf{k}}(\mathbf{r}) \quad (7)$$

$$\hat{S}(\{E|\mathbf{t}\})\hat{S}(\{R|\mathbf{v}\})\psi_{\tau_\beta,\mu,i}^{\mathbf{k}}(\mathbf{r}) = \exp\{-iR\mathbf{k} \cdot \mathbf{t}\}\hat{S}(\{R|\mathbf{v}\})\psi_{\tau_\alpha,\mu,i}^{\mathbf{k}}(\mathbf{r}) \quad (8)$$

i.e., the function $\psi_{\mu,i,\tau_\alpha}^{\mathbf{k}}(\mathbf{r})$ is a Bloch function with wave vector \mathbf{k} and $\hat{S}(\{R|\mathbf{v}\})\psi_{\mu,i,\tau_\alpha}^{\mathbf{k}}(\mathbf{r})$ is a Bloch function with wave vector $R\mathbf{k}$.

The equivalent of Eq.(6) for Zak basis can be written as:

$$\begin{aligned} \hat{S}(\{R|\mathbf{v} + \mathbf{t}\})\Psi_{\tau_\beta,\mu,i}^{\mathbf{k}}(\mathbf{r}) &= \exp\{i[R\mathbf{k} \cdot \tau_\alpha - \mathbf{k} \cdot \tau_\beta]\}\exp\{-iR\mathbf{k} \cdot (\mathbf{v} + \mathbf{t})\} \times \\ &\quad \sum_j D^\mu(R_{\leftarrow}^\tau(R, R_\alpha^\tau))_{ji} \Psi_{\tau_\alpha,\mu,j}^{R\mathbf{k}}(\mathbf{r}). \end{aligned} \quad (9)$$

This expression is the equivalent of Eq.B2 of Ref.[7] or Eq.12 of Ref.[10]. The additional phase factor in the first term compared with those in the literature is significant because absence of such term can change the localisation centres of the Wannier functions through phase shifting theorem. Without these terms, it would not be able to establish the special significance of HSPs.

Neither Eq.(6) nor (9) identify what may occur when \mathbf{k} is at a HSP where $R\mathbf{k}$ may be different from an arm of $\{\mathbf{k}\}$ by a reciprocal lattice vector. To address this, we define some representation matrices to put this formally in group theoretical language. Let $\mathbf{k}, \mathbf{k}' \in \{\mathbf{k}\}$, \mathbf{g}_R be some reciprocal lattice vector including $\mathbf{0}$, and

$$D^{\mathbf{k}}(R)_{\mathbf{k}',\mathbf{k}} = \begin{cases} 1, & \text{if } \mathbf{k}' = R\mathbf{k} - \mathbf{g}_R \\ 0 & \text{otherwise} \end{cases}, \quad D^\tau(R)_{\tau_\alpha,\tau_\beta} = \begin{cases} 1, & \text{if } \{R|\mathbf{v}\}\tau_\beta = \tau_\alpha + \mathbf{t}' \\ 0 & \text{otherwise} \end{cases}, \quad (10)$$

Then Eq.(6) can be expressed as

$$\begin{aligned} \left\langle \mathbf{r} \mid \hat{S}(\{R|\mathbf{v} + \mathbf{t}\}) \mid \mathbf{k}, \tau_\beta, \mu, i \right\rangle_{\text{TB}} &= \hat{S}(\{R|\mathbf{v} + \mathbf{t}\})\psi_{\tau_\beta,\mu,i}^{\mathbf{k}}(\mathbf{r}) \\ &= \sum_{\mathbf{k}' \in \{\mathbf{k}\}} \exp\{-iR\mathbf{k} \cdot (\mathbf{v} + \mathbf{t})\} D^{\mathbf{k}}(R)_{\mathbf{k}',\mathbf{k}} \\ &\quad \sum_{\tau_\alpha} \underbrace{\exp[i\mathbf{g}_R \cdot \tau_\alpha]}_{\text{Gauge Term}} D^\tau(R)_{\tau_\alpha,\tau_\beta} \sum_j D^\mu(R_{\leftarrow}^\tau(R, R_\alpha^\tau))_{ji} \psi_{\tau_\alpha,\mu,j}^{R\mathbf{k}'}(\mathbf{r}) \end{aligned} \quad (11)$$

The term $\exp[i\mathbf{g}_R \cdot \tau_\alpha]$ takes value other than 1 *only* when $\mathbf{g}_R = R\mathbf{k} - \mathbf{k}' \neq \mathbf{0}$. Under this condition, and utilising Eq.(4), Eq.(2)

$$\begin{aligned} \psi_{\tau_\alpha,\mu,j}^{R\mathbf{k}'}(\mathbf{r}) &= \exp[iR\mathbf{k} \cdot \tau_\alpha]\Psi_{\tau_\alpha,\mu,j}^{R\mathbf{k}'}(\mathbf{r}) = \exp[iR\mathbf{k} \cdot \tau_\alpha]\Psi_{\tau_\alpha,\mu,j}^{\mathbf{k}'+\mathbf{g}_R}(\mathbf{r}) = \exp[iR\mathbf{k} \cdot \tau_\alpha]\Psi_{\tau_\alpha,\mu,j}^{\mathbf{k}'}(\mathbf{r}) \\ &= \exp[i(R\mathbf{k} - \mathbf{k}') \cdot \tau_\alpha]\psi_{\tau_\alpha,\mu,j}^{\mathbf{k}'}(\mathbf{r}) = \exp[i\mathbf{g}_R \cdot \tau_\alpha]\psi_{\tau_\alpha,\mu,j}^{\mathbf{k}'}(\mathbf{r}) \end{aligned}$$

For Zak basis, the equivalence of Eq.(11) is obtained using their relation shown in Eq.(4)

$$\begin{aligned}
\left\langle \mathbf{r} \mid \hat{S}(\{R|\mathbf{v} + \mathbf{t}\}) \mid \mathbf{k}, \boldsymbol{\tau}_\beta, \mu, i \right\rangle_{\text{Zak}} &= \hat{S}(\{R|\mathbf{v} + \mathbf{t}\}) \Psi_{\boldsymbol{\tau}_\beta, \mu, i}^{\mathbf{k}}(\mathbf{r}) \\
&= \sum_{\mathbf{k}' \in \{\mathbf{k}\}} \exp\{-iR\mathbf{k} \cdot (\mathbf{v} + \mathbf{t})\} D^{\mathbf{k}}(R)_{\mathbf{k}', \mathbf{k}} \\
&\quad \sum_{\boldsymbol{\tau}_\alpha} \underbrace{\exp\{i[(\mathbf{k}' + \mathbf{g}_R) \cdot \boldsymbol{\tau}_\alpha - \mathbf{k} \cdot \boldsymbol{\tau}_\beta]\}}_{\text{Gauge Term}} D^\tau(R)_{\boldsymbol{\tau}_\alpha, \boldsymbol{\tau}_\beta} \sum_j D^\mu(R_{\leftarrow}^\tau(R, R_\alpha^\tau))_{ji} \Psi_{\boldsymbol{\tau}_\alpha, \mu, j}^{\mathbf{k}'}(\mathbf{r})
\end{aligned} \tag{12}$$

The gauge term is only dependent on wave vector $\mathbf{k}, \mathbf{k}' \in \{\mathbf{k}\}$, the Wyckoff positions $\boldsymbol{\tau}_\alpha, \boldsymbol{\tau}_\beta$, and reciprocal lattice vector \mathbf{g}_R which can be non-zero *only* at HSPs on the surface of Brillouin zone. The existence of the gauge term at HSPs is a consequence of enforcing Eq.(2) for the Zak basis.

The TB bases for a given Wyckoff position is a function of \mathbf{k} and indexed by site symmetry irrep label μ , sub-index i , and site index $\boldsymbol{\tau}_\alpha$ and $\mathbf{k} \in \{\mathbf{k}\}$. Hence the representation matrix of the induced band representation for a general space group element $\{R|\mathbf{v} + \mathbf{t}\}$ is given by

$$\begin{aligned}
\Gamma_{\tilde{G}_\mu^{\tau_\alpha}}^{\mathcal{G}, \text{TB}}(\{R|\mathbf{v} + \mathbf{t}\})_{\mathbf{k}', \boldsymbol{\tau}'_\alpha, i'; \mathbf{k}, \boldsymbol{\tau}_\alpha, i} &= \left\langle \mathbf{k}', \boldsymbol{\tau}'_\alpha, \mu, i' \mid \hat{S}(\{R|\mathbf{v} + \mathbf{t}\}) \mid \mathbf{k}, \boldsymbol{\tau}_\alpha, \mu, i \right\rangle \\
&= \underbrace{\exp[i\mathbf{g}_R \cdot \boldsymbol{\tau}'_\alpha]}_{\Gamma_{\text{gauge}}} \underbrace{D^{\mathbf{k}}(R)_{\mathbf{k}', \mathbf{k}} \exp\{-iR\mathbf{k} \cdot (\mathbf{v} + \mathbf{t})\}}_{\Gamma_{\mathbf{k}}} \underbrace{\{D^\tau(R)_{\boldsymbol{\tau}'_\alpha, \boldsymbol{\tau}_\alpha} \otimes D^\mu(R_{\leftarrow}^\tau(R, R_{\alpha'}^\tau))_{i'i}\}}_{\Gamma_\phi}.
\end{aligned} \tag{13}$$

where $R = R_{\alpha'}^\tau \cdot R_{\leftarrow}^\tau(R, R_{\alpha'}^\tau) \cdot R_{\alpha'}^{\tau-1}$ as detailed in Eq.(A7). It should be emphasised that in writing the direct product in Γ_ϕ , the parameter of the second matrix function $D^\mu(R_{\leftarrow}^\tau(R, R_{\alpha'}^\tau))$ is dependent on the row index of the first matrix function $D^\tau(R)$. The representation matrix naturally separate into three terms: Γ_ϕ which depends on R , Wyckoff position and Wannier function; $\Gamma_{\mathbf{k}}$ which depends on $\{R|\mathbf{v} + \mathbf{t}\}$ and the wave vector \mathbf{k} ; Γ_{Gauge} which exist only on the surface of BZ and dependent on HSPs and Wyckoff position.

Given the Zak basis and TB basis are related by the \mathbf{k} dependent gauge transformation shown in Eq.(4), the band representation for the Zak basis are obtained using the similarity transform as follows:

$$\begin{aligned}
\Gamma_{\tilde{G}_\mu^{\tau_\alpha}}^{\mathcal{G}, \text{Zak}}(\{R|\mathbf{v} + \mathbf{t}\})_{\mathbf{k}', \boldsymbol{\tau}'_\alpha, i'; \mathbf{k}, \boldsymbol{\tau}_\alpha, i} &= \underbrace{\exp\{i[(\mathbf{k}' + \mathbf{g}_R) \cdot \boldsymbol{\tau}'_\alpha - \mathbf{k} \cdot \boldsymbol{\tau}_\alpha]\}}_{\Gamma_{\text{gauge}}} \underbrace{D^{\mathbf{k}}(R)_{\mathbf{k}', \mathbf{k}} \exp\{-iR\mathbf{k} \cdot (\mathbf{v} + \mathbf{t})\}}_{\Gamma_{\mathbf{k}}} \otimes \\
&\quad \underbrace{\{D^\tau(R)_{\boldsymbol{\tau}'_\alpha, \boldsymbol{\tau}_\alpha} \otimes D^\mu(R_{\leftarrow}^\tau(R, R_{\alpha'}^\tau))_{i'i}\}}_{\Gamma_\phi}.
\end{aligned} \tag{14}$$

These analytical representation matrices does not depends on lattice translations generated by $g \in G^\tau$ acting on specific τ as used in the literature^{1,5,7}. Armed with these representation matrices in Eq.(14) and Eq.(13), one can easily project out solutions of desired symmetry at given \mathbf{k} point and compare with solutions obtained from tight binding model constructed from symmetry.

The BR can be decomposed at $\mathbf{k} \in \text{BZ}$ in terms of irreps of $\mathcal{G}^\mathbf{k}$ on restriction to $\mathcal{G}^\mathbf{k}$ (see Sec.IV). Linear combination of the basis of these irreps of $\mathcal{G}^\mathbf{k}$ for $\mathbf{k} \in \{*\mathbf{k}\}$ may form further invariant subspaces under \mathcal{G} . These unitary irreps of \mathcal{G} are identified by $\kappa = \mathbf{k} \in \text{RD}$ and form the nodes in band connectivity. As originally intended by Zak in the use of the term kq representation, the representation is determined explicitly by \mathbf{k} and $\tau_\alpha(q)$ in addition to the irrep labels of the site symmetry group. Its dimension is given by the “the number of arms in star of \mathbf{k} \times the multiplicity of $\tau_\alpha \times d_\mu$ ”. The action of a general space group element $g = \{R|\mathbf{v} + \mathbf{t}\}$ on the basis $|\mathbf{k}, \tau_\alpha, \mu, i\rangle$ of this finite dimensional representation of the space group is to:

1. Permute the wave vector label \mathbf{k} among its $\{*\mathbf{k}\}$,
2. Permute the Wyckoff position label τ_α among its orbit within the primitive cell,
3. Transform the Wannier functions localised on appropriate Wyckoff postions according to element of the site symmetry group.
4. At HSPs on the surface of BZ where $\mathbf{g}_R \neq \mathbf{0}$, the Γ_{Gauge} term modifies the transformation properties.

Comparing the two conventions in defining band representations, they are clearly related by the gauge transformation and may be combined in a single definition with a term $t \in [0, 1]$.

$$\Phi_{\mu,i,\tau_\alpha}^\mathbf{k}(\mathbf{r}) = \Omega^{-1} \sum_\ell \exp\{i\mathbf{k} \cdot (\mathbf{t}_\ell + (1-t)\tau_\alpha)\} \phi_{\tau_\alpha}^{\mu,i}(\mathbf{r} - (\mathbf{t}_\ell + \tau_\alpha)).$$

Here $t = 0$ correspond to the TB band representation and $t = 1$ correspond to the Zak band representation.

An alternative view of this, through the phase shifting theorem of Fourier transform and with sampling as per TB basis, is the following:

$$\Phi_{\mu,i,\tau_\alpha}^\mathbf{k}(\mathbf{r}) = \Omega^{-1} \sum_\ell \exp\{i\mathbf{k} \cdot (\mathbf{t}_\ell + \tau_\alpha)\} \phi_{\tau_1}^{\mu,i}(\mathbf{r} - (\mathbf{t}_\ell + \tau_\alpha - t\tau_\alpha)).$$

Again, we recover the TB basis at $t = 0$, and Zak basis at $t = 1$. Which ever view one takes, the Wyckoff position is explicit in the basis definition. This alternative view via phase shifting theorem allows equivalent band representation to be considered. It also shows the potential impact of missing phase term in the literature as it would lead to shifting of localisation centres of Wannier functions.

A final remark about PEGRs. To incorporate the effect of spin, it is necessary to make use of Wannier functions which transforms according to the double group basis of the site symmetry group. The inter-site spin dependent effect is then generated by the appropriate \mathbf{k} dependence of the band representation. For example, the opening of bulk gap at K point in graphene.

III. GROUP THEORETICAL BASIS OF TIGHT BINDING THEORY

In tight binding theory, the basis used to express the wave function are the Bloch sums shown in Eq.(3) or (1). Yet the evaluation of the tight binding model are performed via sequential sums over ‘atoms’ (Wyckoff positions) on shells of the same radius. This clearly indicate that the translational symmetry must be factored out in the evaluation of the matrix element.

First of all, basis of representations of space group \mathcal{G} derived from any band representations but at *different* wave vectors are orthogonal, i.e.

$$\langle \mathbf{k}', \sigma_\alpha, \mu, i | \mathbf{k}, \tau_\alpha, \nu, j \rangle = 0, \quad \text{unless } \mathbf{k}' = \mathbf{k} + \mathbf{K}_n.$$

Since \mathcal{G} is the symmetry group of the Hamiltonian operator \hat{H} , its matrix representation with respect to such basis are zero unless the wave vectors are the same. From group rearrangement theorem, its matrix representation are given by

$$\begin{aligned} \langle \mathbf{k}, \sigma_\alpha, \mu, i | \hat{H} | \mathbf{k}, \tau_\beta, \nu, j \rangle &= \frac{1}{|\mathcal{G}|} \sum_{g \in \mathcal{G}} g \bullet \langle \mathbf{k}, \sigma_\alpha, \mu, i | \hat{H} | \mathbf{k}, \tau_\beta, \nu, j \rangle \\ &= \frac{1}{|\mathcal{G}|} \sum_{g \in \mathcal{G}} \left\langle \mathbf{k}, \sigma_\alpha, \mu, i | \hat{S}(g)^\dagger \underbrace{\hat{S}(g) \hat{H} \hat{S}(g)^\dagger}_{=\hat{H}} \hat{S}(g) | \mathbf{k}, \tau_\beta, \nu, j \right\rangle \\ &= \frac{1}{|\mathcal{G}|} \sum_{g \in \mathcal{G}} \langle \mathbf{k}, \sigma_\alpha, \mu, i | \hat{S}(g)^\dagger \hat{H} \hat{S}(g) | \mathbf{k}, \tau_\beta, \nu, j \rangle \end{aligned} \quad (15)$$

which refers to the full matrix representation with row and column indexed by distinct $\mathbf{k} \in \{\mathbf{k}\}, \sigma_\alpha, \mu, i$ labels. The multiplicity of the of σ_α and τ_β are m and n respectively. A

quick conclusion can be made from Eq.(15). If we act on both side by an element $\{R|\mathbf{v} + \mathbf{t}\}$ which permute \mathbf{k} index among $\{*\mathbf{k}\}$, the \mathbf{k} index on the LHS would change, yet the RHS remains unchanged due to group rearrangement theorem. Hence each diagonal sub block indexed by $\mathbf{k}' \in \{*\mathbf{k}\}$ have the same functional dependence on \mathbf{k} and form. The off-diagonal blocks must be zero.

Given the partition of \mathcal{G} in terms of the left cosets of \mathcal{T} in Eq.(A1), any space group element can be expressed uniquely as the product of a coset representative and an element of the translation sub-group

$$\{R_i|\mathbf{v}_i + \mathbf{t}'\} = \{R_i|\mathbf{v}_i\} \cdot \{E|R^{-1}\mathbf{t}'\} = \{R_i|\mathbf{v}_i\} \cdot \{E|\mathbf{t}\}$$

Hence the summation over \mathcal{G} can be separated into summation over \mathcal{T} and the summation over the coset representatives in Eq.(A1),

$$\begin{aligned} \langle \mathbf{k}, \boldsymbol{\sigma}_\alpha, \mu, i | \hat{H} | \mathbf{k}, \boldsymbol{\tau}_\beta, \nu, j \rangle &= \frac{1}{|\mathcal{F}||\mathcal{T}|} \sum_{g=\{R_i|\mathbf{v}_i\}:R_i \in \mathcal{F}} \sum_{\{E|\mathbf{t}\} \in \mathcal{T}} \\ &\quad \langle \mathbf{k}, \boldsymbol{\sigma}_\alpha, \mu, i | \hat{S}(\{E|\mathbf{t}\})^\dagger \hat{S}(g)^\dagger \hat{H} \hat{S}(g) \hat{S}(\{E|\mathbf{t}\}) | \mathbf{k}, \boldsymbol{\tau}_\beta, \nu, j \rangle \\ &= \frac{1}{|\mathcal{F}||\mathcal{T}|} \sum_{g=\{R_i|\mathbf{v}_i\}:R_i \in \mathcal{F}} \sum_{\mathbf{t} \in \mathcal{T}} \exp(i\mathbf{k} \cdot \mathbf{t}) \langle \mathbf{k}, \boldsymbol{\sigma}_\alpha, \mu, i | \hat{S}(g)^\dagger \hat{H} \hat{S}(g) | \mathbf{k}, \boldsymbol{\tau}_\beta, \nu, j \rangle \exp(-i\mathbf{k} \cdot \mathbf{t}) \\ &= \frac{1}{|\mathcal{F}|} \sum_{g=\{R_i|\mathbf{v}_i\}:R_i \in \mathcal{F}} \langle \mathbf{k}, \boldsymbol{\sigma}_\alpha, \mu, i | \hat{S}(g)^\dagger \hat{H} \hat{S}(g) | \mathbf{k}, \boldsymbol{\tau}_\beta, \nu, j \rangle \end{aligned} \quad (16)$$

Thus the summation over all space group elements is reduced to summation over the coset representatives in partition of \mathcal{G} in Eq.(A1). If we were to implement the transformation properties of band representation as per Eq.(6), the dependence on non-lattice translations in the coset representatives will also disappear. Hence the matrix representations of the Hamiltonian with respect to the TB basis are determined by the elements of point group of the crystal. This does not imply that the point group \mathcal{F} is a sub-group of \mathcal{G} . In deriving Eq.(16), an assumption of invariance of \hat{H} is assumed. Whilst the explicit form of the matrix representation of the Hamiltonian is not dependent on the non-lattice translation in $\{R_i|\mathbf{v}_i\}$, the invariance of \hat{H} requires the non-lattice translation. On the other had, the summation over the coset representative does not require them to form a group.

To extract the \mathbf{k} dependence, we have to evaluate Eq.(16) with the definition of TB basis in Eq.(3). Instead of considering the infinite sum over all Wannier functions leading to the rotation of wave-vector \mathbf{k} , we focus on a subset of terms but leaving the wave-vector

constant. Specifically, we need to consider subset of all Wannier functions which are reached from a Wannier functions centred on $(\mathbf{t}'_\ell + \boldsymbol{\tau}_\beta)$ under the action of coset representatives. The sum over all lattice vectors in Eq.(3) can then be partitioned into sum over *sets of terms reached under the operation of coset representatives*. For atomic positions indicated by $\mathbf{t}_\ell + \boldsymbol{\sigma}_\alpha$ and $\mathbf{t}'_\ell + \boldsymbol{\tau}_\beta$, we define sets of centres of Wannier functions reached under the action of coset representatives as,

$$\mathcal{A} = \{(\mathbf{t}'' + \boldsymbol{\sigma}_\gamma) = \{R_i|\mathbf{v}_i\}(\mathbf{t}_\ell + \boldsymbol{\sigma}_\alpha) \mid \forall R_i \in \mathcal{F}\} \quad (17a)$$

$$\mathcal{B} = \{(\mathbf{t}''' + \boldsymbol{\tau}_\delta) = \{R_i|\mathbf{v}_i\}(\mathbf{t}'_\ell + \boldsymbol{\tau}_\beta) \mid \forall R_i \in \mathcal{F}\} \quad (17b)$$

Consider the transformation properties of a typical Wannier function in the TB basis centred at $\mathbf{t}'_\ell + \boldsymbol{\tau}_\beta$. Using the terms defined in Eq.(10)

$$\begin{aligned} \langle \mathbf{r} \mid \hat{S}(\{R|\mathbf{v}\}) \mid (\mathbf{t}'_\ell + \boldsymbol{\tau}_\beta), \nu, j \rangle &= \hat{S}(\{R|\mathbf{v}\}) \phi_{\nu,i}^{\boldsymbol{\tau}_\beta}(\mathbf{r} - (\mathbf{t}'_\ell + \boldsymbol{\tau}_\beta)) \\ &= \sum_{(\mathbf{t}'''_\ell + \boldsymbol{\tau}_\delta) \in \mathcal{B}} D^\tau(R)_{\boldsymbol{\tau}_\delta, \boldsymbol{\tau}_\beta} \sum_q D^\nu(R_{\leftarrow}^\tau(R, R_\delta^\tau))_{qj} \phi_{\nu,q}^{\boldsymbol{\tau}_\delta}(\mathbf{r} - (\mathbf{t}'''_\ell + \boldsymbol{\tau}_\delta)) \end{aligned}$$

where $R_{\leftarrow}^\tau(R, R_\delta^\tau)$ is determined by Eq.(A7). We define representation matrices

$$D^{\tau,\nu}(R) = D^\tau(R) \otimes D^\nu(R_{\leftarrow}^\tau(R, R_\delta^\tau)).$$

Thus

$$\hat{S}(\{R|\mathbf{v}\}) \phi_{\nu,j}^{\boldsymbol{\tau}_\beta}(\mathbf{r} - (\mathbf{t}'_\ell + \boldsymbol{\tau}_\beta)) = \sum_{(\mathbf{t}'''_\ell + \boldsymbol{\tau}_\delta) \in \mathcal{B}} \sum_q D^{\tau,\nu}(R)_{\boldsymbol{\tau}_\delta, q; \boldsymbol{\tau}_\beta, j} \phi_{\nu,q}^{\boldsymbol{\tau}_\delta}(\mathbf{r} - (\mathbf{t}'''_\ell + \boldsymbol{\tau}_\delta)) \quad (18)$$

For a given Wannier function centred at $\mathbf{t}'_\ell + \boldsymbol{\tau}_\beta$, a set of basis functions of the form

$$\langle r \mid \mathbf{k}, (\mathbf{t}'''_\ell + \boldsymbol{\tau}_\delta), \nu, j \rangle = \exp[i\mathbf{k} \cdot (\mathbf{t}'''_\ell + \boldsymbol{\tau}_\delta)] \phi_{\nu,i}^{\boldsymbol{\tau}_\delta}(r - (\mathbf{t}'''_\ell + \boldsymbol{\tau}_\delta)), \quad \forall (\mathbf{t}'''_\ell + \boldsymbol{\tau}_\delta) \in \mathcal{B} \quad (19)$$

can be reached from the action of the coset representatives. Similar set can be constructed for Wannier functions centred at $\mathbf{t}_\ell + \boldsymbol{\sigma}_\alpha$. They constitute a subset of terms in the Bloch sum of Eq.(3). The sum over all Wannier functions in Eq.(3) are partitioned into such set reached from $\mathbf{t}'_\ell + \boldsymbol{\tau}_\beta$. We shall show that such partition is mutually exclusive. The form of the matrix representation for the Hamilton, including explicit \mathbf{k} dependance, are determined for each partition of the lattice sum for the bra and ket respectively. The \mathbf{k} dependence is clearly different for each closed set arising from the different phase factors above.

For a particular partitions defined by \mathbf{k} , $\mathbf{t}_\ell + \boldsymbol{\sigma}_\alpha$, μ , i , $\mathbf{t}'_\ell + \boldsymbol{\tau}_\beta$, ν , j , the sum over coset representatives in Eq.(16) can then be written as

$$\begin{aligned} \left\langle \mathbf{k}, \mathbf{t}_\ell + \boldsymbol{\sigma}_\alpha, \mu, i \mid \hat{H} \mid \mathbf{k}, \mathbf{t}'_\ell + \boldsymbol{\tau}_\beta, \nu, j \right\rangle &= \frac{1}{|\mathbf{F}|} \sum_{R_i \in \mathbf{F}} \sum_{(\mathbf{t}'_\ell + \boldsymbol{\sigma}_\gamma) \in \mathcal{A}} \sum_{(\mathbf{t}'''_\ell + \boldsymbol{\tau}_\delta) \in \mathcal{B}} \sum_p \sum_q \\ \left\langle \mathbf{k}, (\mathbf{t}''_\ell + \boldsymbol{\sigma}_\gamma), \mu, p \mid \hat{H} \mid \mathbf{k}, (\mathbf{t}'''_\ell + \boldsymbol{\tau}_\delta), \nu, q \right\rangle D^{\boldsymbol{\sigma}, \mu}(R)_{\boldsymbol{\sigma}_\gamma, p; \boldsymbol{\sigma}_\alpha, i}^* D^{\boldsymbol{\tau}, \nu}(R)_{\boldsymbol{\tau}_\delta, q; \boldsymbol{\tau}_\beta, j} \end{aligned}$$

Restoring the explicit \mathbf{k} dependence on the RHS for this partition,

$$\begin{aligned} \left\langle \mathbf{k}, \mathbf{t}_\ell + \boldsymbol{\sigma}_\alpha, \mu, i \mid \hat{H} \mid \mathbf{k}, \mathbf{t}'_\ell + \boldsymbol{\tau}_\beta, \nu, j \right\rangle &= \frac{1}{|\mathbf{F}|} \sum_{R_i \in \mathbf{F}} \sum_{(\mathbf{t}'_\ell + \boldsymbol{\sigma}_\gamma) \in \mathcal{A}} \sum_{(\mathbf{t}'''_\ell + \boldsymbol{\tau}_\delta) \in \mathcal{B}} \exp\{i\mathbf{k} \cdot [(\mathbf{t}'''_\ell + \boldsymbol{\tau}_\delta) - (\mathbf{t}''_\ell + \boldsymbol{\sigma}_\gamma)]\} \\ &\quad \sum_p \sum_q \left\langle (\mathbf{t}''_\ell + \boldsymbol{\sigma}_\gamma), \mu, p \mid \hat{H} \mid (\mathbf{t}'''_\ell + \boldsymbol{\tau}_\delta), \nu, q \right\rangle D^{\boldsymbol{\sigma}, \mu}(R)_{\boldsymbol{\sigma}_\gamma, p; \boldsymbol{\sigma}_\alpha, i}^* D^{\boldsymbol{\tau}, \nu}(R)_{\boldsymbol{\tau}_\delta, q; \boldsymbol{\tau}_\beta, j} \end{aligned}$$

Here the vectors $(\mathbf{t}'''_\ell + \boldsymbol{\tau}_\delta)$ and $(\mathbf{t}''_\ell + \boldsymbol{\sigma}_\gamma)$ are related to the original chosen centres of Wannier function by the action of the coset representatives. Hence there differences are given by:

$$\begin{aligned} (\mathbf{t}'''_\ell + \boldsymbol{\tau}_\delta) - (\mathbf{t}''_\ell + \boldsymbol{\sigma}_\gamma) &= \{R|\mathbf{v}\}(\mathbf{t}'_\ell + \boldsymbol{\tau}_\beta) - \{R|\mathbf{v}\}(\mathbf{t}_\ell + \boldsymbol{\sigma}_\alpha) \\ &= R[(\mathbf{t}'_\ell + \boldsymbol{\tau}_\beta) - (\mathbf{t}_\ell + \boldsymbol{\sigma}_\alpha)] \quad \exists R \in \mathbf{F}. \end{aligned}$$

Setting $\boldsymbol{\rho}_1 = (\mathbf{t}'_\ell + \boldsymbol{\tau}_\beta) - (\mathbf{t}_\ell + \boldsymbol{\sigma}_\alpha)$, the action of coset representatives generates N ($N \leq |\mathbf{F}|$) independent vectors $\boldsymbol{\rho}_1, \dots, \boldsymbol{\rho}_N$, *all having the same magnitude as $|\boldsymbol{\rho}_1|$* . As the rotational part of the coset representatives form the group \mathbf{F} , the set of phase factor $\exp[i\mathbf{k} \cdot \boldsymbol{\rho}_r]$ form the basis of a representation of the point group. We may express

$$\exp[i\mathbf{k} \cdot (\mathbf{t}'''_\ell + \boldsymbol{\tau}_\delta) - (\mathbf{t}''_\ell + \boldsymbol{\sigma}_\gamma)] = \sum_r D^\rho(R)_{r1} \exp[i\mathbf{k} \cdot \boldsymbol{\rho}_r] \quad (20)$$

Hence the sum over the partitions of terms in TB basis in Eq.(16) can be expressed as

$$\begin{aligned} \left\langle \mathbf{k}, \mathbf{t}_\ell + \boldsymbol{\sigma}_\alpha, \mu, i \mid \hat{H} \mid \mathbf{k}, \mathbf{t}'_\ell + \boldsymbol{\tau}_\beta, \nu, j \right\rangle &= \frac{1}{|\mathbf{F}|} \sum_{R_i \in \mathbf{F}} \sum_r D^\rho(R)_{r1} \sum_{(\mathbf{t}'_\ell + \boldsymbol{\sigma}_\gamma) \in \mathcal{A}} \sum_p D^{\boldsymbol{\sigma}, \mu}(R)_{\boldsymbol{\sigma}_\gamma, p; \boldsymbol{\sigma}_\alpha, i}^* \\ &\quad \sum_{(\mathbf{t}'''_\ell + \boldsymbol{\tau}_\delta) \in \mathcal{B}} \sum_q D^{\boldsymbol{\tau}, \nu}(R)_{\boldsymbol{\tau}_\delta, q; \boldsymbol{\tau}_\beta, j} \exp[i\mathbf{k} \cdot \boldsymbol{\rho}_r] \left\langle (\mathbf{t}''_\ell + \boldsymbol{\sigma}_\gamma), \mu, p \mid \hat{H} \mid (\mathbf{t}'''_\ell + \boldsymbol{\tau}_\delta), \nu, q \right\rangle \quad (21) \end{aligned}$$

Eq.(21) shows that the transformation of the matrix representation of the Hamiltonian with respect to the subset of terms in the TB basis is a direct product of the three representations of the point group $D^\rho(R) \otimes D^{\boldsymbol{\sigma}, \mu}(R)^* \otimes D^{\boldsymbol{\tau}, \nu}(R)$. The non-lattice translation associated with the coset representatives does not appear in the transformation properties. The LHS of Eq.(21) will only be non-zero if $\Gamma_1 \in D^\rho(R) \otimes D^{\boldsymbol{\sigma}, \mu}(R)^* \otimes D^{\boldsymbol{\tau}, \nu}(R)$. We can, therefore treat

this as a projection operator for the trivial representation and obtain the explicit form except for a number of material dependent constant for this partition.

The hierarchy of dictionary order of the projected column matrix is $\rho_r, \sigma_\alpha, i, \tau_\beta, j$ as it is written in Eq.(21). The limited space spanned by the set of Wannier functions in (19) may not support all the symmetry permitted form. To project out all the correct and linearly independent forms, one should start with a trial vector with non-zero entries in the sub-space set by $\rho_1, \sigma_\alpha, \tau_\beta$ (i.e. those corresponding to LHS of Eq.(21)) or any other set generated by the action of the coset representatives. The space of i and j need to be explored for linearly independent forms.

A few remarks about the result in Eq.(21).

1. The enumeration of the centres of Wannier functions in Eq.(17), and bases in Eq.(19) would generate all the equivalent Wyckoff position in σ_α and τ_β . Therefore Eq.(21) determines the contribution to the $(m \times d_\mu) \times (n \times d_\nu)$ H matrix from the partition of Wannier functions for a given wave-vector \mathbf{k} .
2. Whilst the generation of centres of Wannier function from the chosen vector $(\mathbf{t}'_\ell + \tau_\beta)$ in Eq.(17) is by the coset representative (thus it may not be closed since the coset representative does not necessarily form a group), the set of difference vectors $\rho_r = (\mathbf{t}'''_\ell + \tau_\delta) - (\mathbf{t}''_\ell + \sigma_\gamma)$ are closed under the action of rotational part of the coset representatives, or elements of the point group F. There could be no other vector $|\rho'| = |(\mathbf{t}' - \tau) - (\mathbf{t} - \sigma)| = |\rho_1|$, other than a lattice translated copy of ρ_r since we have exhausted all the coset representatives in Eq.(17). Hence the partition of sums over all Wannier functions in Eq.(3) according to sets in Eq.(17) is unique and complete for the purpose of evaluating Eq.(16). i.e. all terms in Eq.(3) occurs in one and only one partition for the purpose of evaluating Eq.(16).
3. The non-lattice translation in the coset representative is again absent in the final result. Therefore the explicit form of the matrix representation of Hamiltonian with respect to each partition is determined by the properties of the point group only. As stated before, whilst the form of the Hamiltonian is fixed by the elements of the point group, the derivation clearly requires the use of full space group element. I
4. Since Eq.(21) is obtained without referring to the nature of the interaction between the

Wannier orbitals, it takes into account the two centre interaction in the Slater-Koster theory as well as all other symmetry permitted interactions. This also include perturbative effect of other orbitals excluded in the consideration through quasi-degenerate perturbation theory. Specifically, this includes the spin dependent term in second nearest neighbour interaction²⁶ which give rise to the band gap in graphene and the non-trivial band topology (see Sec.V).

5. The maximum number of linearly independent projection result (and invariant material parameters) for a given set is the number of trivial representation of F contained in the triple product of $D^\rho(R) \otimes D^{\sigma,\mu}(R)^* \otimes D^{\tau,\nu}(R)$ contained in Eq.(21). Those contained in the partition defined by the starting ρ_1 , σ_α , τ_β can be obtained by exploring i and j space.

Appendix B gives an example of using Eq.(21) to derive tight binding model for p_z orbitals in single layer graphene to second nearest neighbours. There have been implicit use of group theory in formulating TB Hamiltonian, for example Eq.(2) of Ref.[20]. Without assessing the correctness of the Hamiltonian, the Hermitian conjugate terms are already generated by the action of point group elements. Their explicit inclusion would lead to double counting. A systematic approach here generates all the symmetry permitted terms with appropriate interaction parameters.

IV. DECOMPOSITION OF BAND REPRESENTATION AT \mathbf{k}

At a given wave vector $\mathbf{k} \in RD$, the BR form a representation of \mathcal{G} which is generally reducible. In utilising BR, we are frequently interested in its decomposition into irreps of \mathcal{G} . The latter is generally obtained from representation induced from irrep of \mathcal{G}^k . The BR also form a subduced representation of \mathcal{G}^k which is generally reducible. By Frobenius reciprocity theorem, the decomposition of BR @ $\mathbf{k} \in RD$ in terms of irreps of \mathcal{G} is obtained from decomposition of subdueed representation in terms of irreps of \mathcal{G}^k . Much of the theory on induced representation of space group is covered in chapter 4 of Ref.[22]. For this purpose, the irreps of \mathcal{G}^k is induced from irreps of its co-group $\tilde{\mathcal{G}}^k$. Its matrix of representation of \mathcal{G}^k induced from irrep p of $\tilde{\mathcal{G}}^k$ is given by:²²

$$\Gamma_{\tilde{\mathcal{G}}_p^k}^{\mathcal{G}^k}(\{R|\mathbf{v} + \mathbf{t}\}) = \exp\{-i\mathbf{k} \cdot (\mathbf{v} + \mathbf{t})\} D_p^k(R), \quad \{R|\mathbf{v} + \mathbf{t}\} \in \mathcal{G}^k \quad (22)$$

These are used to induce representations of space group \mathcal{G} . The irreducibility of such induced representation is determined by Mackey's or Johnston's irreducibility criterion²². Implicit in this process is the requirement of the gauge condition in Eq.(2) except where projective representation occur in the case of non-symmorphic space group. The choice of Eq.(22) is not very convenient for intended decomposition because of the differing dependence of \mathbf{k} and $R\mathbf{k}$ in the exponent containing $\mathbf{v} + \mathbf{t}$. There is an alternative choice for the representation matrices as

$$\Gamma_{\tilde{G}_p^k \uparrow}^{G^k}(\{R|\mathbf{v} + \mathbf{t}\}) = \exp\{-iR\mathbf{k} \cdot (\mathbf{v} + \mathbf{t})\} D_p^k(R), \quad \{R|\mathbf{v} + \mathbf{t}\} \in \mathcal{G}^k \quad (23)$$

The situation where $R\mathbf{k}$ differs from \mathbf{k} can only occur at HSPs on the surface of the BZ. One can see the equivalence of the two through the following. The difference between the two expression is given by $\exp\{i\mathbf{g}_R \cdot (\mathbf{v} + \mathbf{t})\}$ where $R\mathbf{k} - \mathbf{k} = \mathbf{g}_R \neq 0$ can only occur on HSP on the surface of BZ. For symmorphic space groups, $\mathbf{v} = \mathbf{0}$ and the term returns 1 irrespective the value of \mathbf{g}_R (reciprocal lattice vector). For non-symmorphic space group and where $\mathbf{g}_R = 0$, the term also returns 1. The only remaining case is non-symmorphic space group at HSP on the surface of BZ where projective representation is required. Specifically Eq.(22) yields factoring system

$$D_p^k(R_i)D_p^k(R_j) = \exp[i(\mathbf{g}_i \cdot R_i \mathbf{v}_j)] D_p^k(R_k) \quad \text{where } R_i \mathbf{k} - \mathbf{k} = \mathbf{g}_i$$

where as Eq.(23) yields

$$D_p^k(R_i)D_p^k(R_j) = \exp\{i[\mathbf{g}_i \cdot (\mathbf{v}_i + R_i \mathbf{v}_j) + \mathbf{g}_j \cdot \mathbf{v}_j - \mathbf{g}_k \cdot \mathbf{v}_k]\} D_p^k(R_k).$$

We wish to examine the decomposition of the subduced band representation at given \mathbf{k} into irreducible form upon restriction to \mathcal{G}^k . For this purpose, it is easier to make the choice of Eq.(23) as irreducible representation of \mathcal{G}^k . This will allow the irreps of \mathcal{G}^k to share the same dependence on translation as the BR and factoring out many of the summation over \mathcal{T} we will encounter. We need to work with the Zak basis as it satisfy the gauge condition in Eq.(2). (The characters obtained from the TB band representation is the same as the Zak representation. So from decomposition perspective, it does not matter which convention to use. But Zak basis must be used when projection operators is constructed)

The character of the irrep of \mathcal{G}^k shown in Eq.(23) is:

$$\chi_{\tilde{G}_p^k \uparrow}^{G^k}(\{R|\mathbf{v} + \mathbf{t}\}) = \exp\{-iR\mathbf{k} \cdot (\mathbf{v} + \mathbf{t})\} \chi_{\tilde{G}^k}^p(R), \quad \{R|\mathbf{v} + \mathbf{t}\} \in \mathcal{G}^k \quad (24)$$

From Eq.(14), the character of the subduced Zak BR, on restriction to \mathbf{k} and $\mathcal{G}^{\mathbf{k}}$ is given by:

$$\begin{aligned} \chi_{\mathcal{G}(\tilde{\mathbf{G}}_{\mu}^{\tau}\uparrow)\downarrow}^{\mathcal{G}^{\mathbf{k}}}(\{R|\mathbf{v} + \mathbf{t}\}) &= \exp\{-R\mathbf{k} \cdot (\mathbf{v} + \mathbf{t})\} \\ \sum_{\tau_{\alpha}} \delta_{\tau_{\alpha}, \{R|\mathbf{v} + \mathbf{t}\}\tau_{\alpha}} \exp\{i\mathbf{g}_R \cdot \tau_{\alpha}\} \chi_{\tilde{\mathbf{G}}^{\tau}}^{\mu}(R_{\alpha}^{\tau-1}RR_{\alpha}^{\tau}) & \quad \{R|\mathbf{v} + \mathbf{t}\} \in \mathcal{G}^{\mathbf{k}} \end{aligned} \quad (25)$$

where $R\mathbf{k} - \mathbf{k} = \mathbf{g}_R$ can take the value of $\mathbf{0}$ or some reciprocal lattice vector (for some HSP on the surface of BZ and certain $R \in \tilde{\mathbf{G}}^{\mathbf{k}}$)

The decomposition theorem gives the multiplicity of irrep $\Gamma_{\tilde{\mathbf{G}}_{\mu}^{\tau}\uparrow}^{\mathcal{G}^{\mathbf{k}}}$ contained in $\Gamma_{\mathcal{G}(\tilde{\mathbf{G}}_{\mu}^{\tau}\uparrow)\downarrow}^{\mathcal{G}^{\mathbf{k}}}$

$$\begin{aligned} a &= \frac{1}{|\mathcal{G}^{\mathbf{k}}|} \sum_{\{R|\mathbf{v} + \mathbf{t}\} \in \mathcal{G}^{\mathbf{k}}} \chi_{\tilde{\mathbf{G}}_{\mu}^{\tau}\uparrow}^{\mathcal{G}^{\mathbf{k}}}(\{R|\mathbf{v} + \mathbf{t}\})^* \chi_{\mathcal{G}(\tilde{\mathbf{G}}_{\mu}^{\tau}\uparrow)\downarrow}^{\mathcal{G}^{\mathbf{k}}}(\{R|\mathbf{v} + \mathbf{t}\}) \\ &= \frac{1}{|\mathcal{G}^{\mathbf{k}}|} \sum_{\{R|\mathbf{v} + \mathbf{t}\} \in \mathcal{G}^{\mathbf{k}}} \chi_{\tilde{\mathbf{G}}^{\mathbf{k}}}(R)^* \sum_{\tau_{\alpha}} \delta_{\tau_{\alpha}, \{R|\mathbf{v} + \mathbf{t}\}\tau_{\alpha}} \exp\{i\mathbf{g}_R \cdot \tau_{\alpha}\} \chi_{\tilde{\mathbf{G}}^{\tau}}^{\mu}(R_{\alpha}^{\tau-1}RR_{\alpha}^{\tau}) \end{aligned}$$

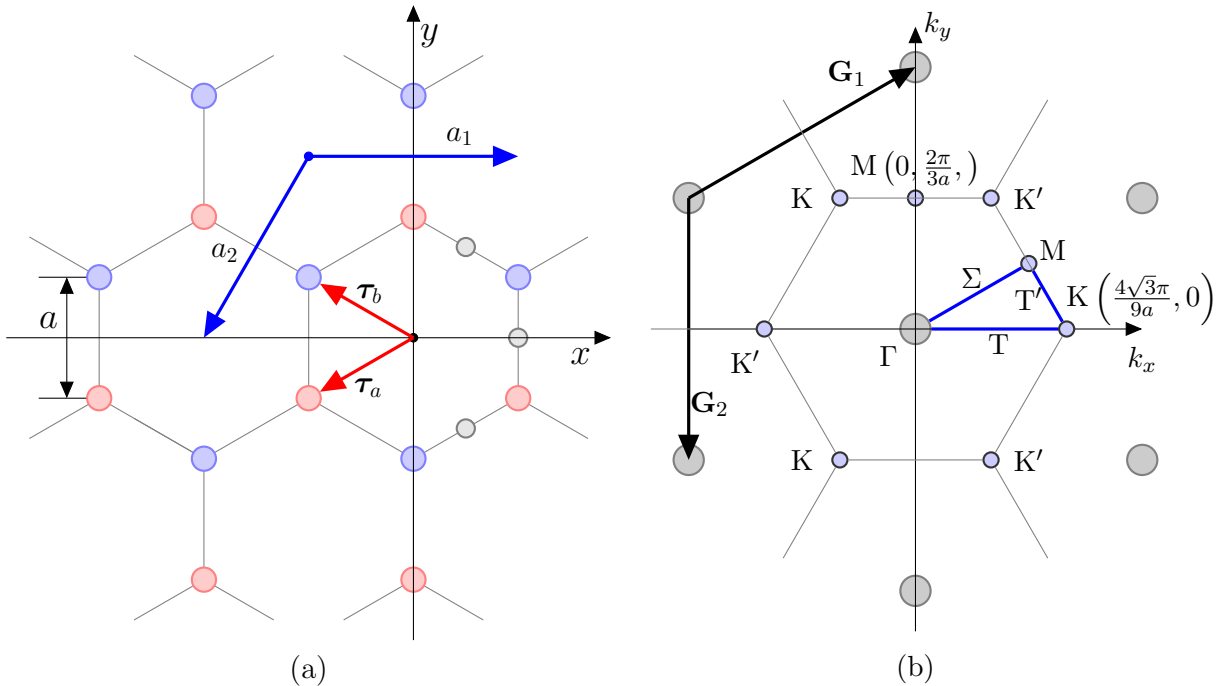


FIG. 1. (a) Honeycomb lattice indicating the position of Wyckoff position 2c and 3f, and (b) first Brillouin zone in reciprocal space.

The summation over the translation sub-group is factored out, giving

$$a = \frac{1}{|\tilde{G}^k|} \sum_{R \in \tilde{G}^k} \chi_{\tilde{G}^k}^p(R)^* \underbrace{\sum_{\tau_\alpha} \delta_{\tau_\alpha, \{R|\mathbf{v}\}\tau_\alpha} \exp\{i\mathbf{g}_R \cdot \tau_\alpha\} \chi_{\tilde{G}^\tau}^\mu(R_\alpha^{\tau^{-1}} R R_\alpha^\tau)}_{\chi_\phi(R)}, \quad R \in \tilde{G}^k. \quad (26)$$

For a given element of $R \in \tilde{G}^k$, its mapping to $R_\alpha^{\tau^{-1}} R R_\alpha^\tau \in \tilde{G}^\tau$ are to the same conjugacy class in \tilde{G}^τ for different τ_α where $\delta_{\tau_\alpha, \{R|\mathbf{v}+\mathbf{t}\}\tau_\alpha} = 1$. The decomposition of BR at $\mathbf{k} \in \text{RD}$ in terms of irreps of \mathcal{G} is then obtained through Frobenius reciprocity theorem.

With the exception of high symmetry points on the surface of the Brillouin zone where $R\mathbf{k} - \mathbf{k} = \mathbf{g}_R \neq \mathbf{0}$, the decomposition is fixed everywhere in the Brillouin zone once the decomposition at Γ point is specified. Thus to establish the equivalence of band representations, we need to establish *the same decomposition at Γ point as well as all other high symmetry points on the surface of the Brillouin zone where $R\mathbf{k} - \mathbf{k} = \mathbf{g}_R \neq \mathbf{0}$ occurs*. The decomposition rule here is much simpler than those stated in the original publication defining the band representations¹.

Here we perform a decomposition analysis of band representations induced from various localised orbitals on Wyckoff position 2c (including p_z), 3f and 1a on honeycomb lattice with symmorphic space group 191²⁸. This lattice is also described by layer group 80²⁹. The choice of this space naturally prohibit the Rashba term which is not a integral part of honeycomb lattice and breaks inversion symmetry. We follow the designation of point group irreps as in KDWS³⁰. The site symmetry group of the Wyckoff poisions 2c and 3f are isomorphic to the point group D_{3h} and D_{2h} respectively. The point group assoicated with this space group is D_{6h} . Specifically, the p_z orbital on Wyckoff position 2c has the symmetry of Γ_4 without spin and Γ_8 with spin under the site symmetry group. The real and reciprocal space representation, with appropriate basis vectors and labels are shown in Fig.1. Tab.I shows the relationship between the operations of the little co-group of \mathbf{k} at high symmetry points and operations of the site symmetry group, and lists the character χ_ϕ as shown in Eq.(26). Where $R\mathbf{k} - \mathbf{k} = \mathbf{g}_R \neq \mathbf{0}$ occurs (labelled by operation in \tilde{G}^k in coloured background), the χ_ϕ modified by the gauge term is shown in bracket.

Using Eq.(26), the decomposition of band representations in terms of irreps of \mathcal{G}^k induced from irreps of \tilde{G}^k are obtained and shown in Tab.II. At K, T', and M point, $R\mathbf{k} - \mathbf{k}$ may take non-zero value in \mathbf{g}_R but only the C_3 & S_3 types of operations for K point lead to a change of character of the conjugacy classes for Wyckoff position 2c. In contrast, many more

TABLE I. Characters Γ_ϕ^T of the band representation on restriction to \mathcal{G}^k . The local orbitals are centred on Wyckoff positions 2c, or 3f of $\mathcal{G} = 80(L)/191(S)$. The operation of $\tilde{\mathcal{G}}^k$ at high symmetry points in the Brillouin zone are indicated. Where the character is modified by the gauge term, it is shown in bracket.

$\tilde{\mathcal{G}}^k$		$\Gamma(D_{6h})$	$\{E\}$	$\{2C_6\}$	$\{2C_3\}$	$\{C_2\}$	$\{3C'_2\}$	$\{3C''_2\}$	$\{i\}$	$\{2S_3\}$	$\{2S_6\}$	$\{\sigma_h\}$	$\{3\sigma_d\}$	$\{3\sigma_v\}$
		T(C_{2v})	$\{E\}$	-	-	-	-	$\{C_2\}$	-	-	-	$\{\sigma_v\}$	$\{\sigma'_v\}$	-
2c	K(D_{3h})	$\{E\}$	-	$\{2C_3\}$		-	-	$\{3C_2\}$	-	$\{2S_3\}$	-	$\{\sigma_h\}$	$\{3\sigma_v\}$	-
	T'(C_{2v})	$\{E\}$	-	-	-	-	-	$\{C_2\}$	-	-	-	$\{\sigma_v\}$	$\{\sigma'_v\}$	-
	M(D_{2h})	$\{E\}$	-	-	$\{C_2\}$	$\{C'_2\}$	$\{C''_2\}$	$\{i\}$	-	-	$\{\sigma_h\}$	$\{\sigma_v\}$	$\{\sigma'_v\}$	
	$\Sigma(C_{2v})$	$\{E\}$	-	-	-	$\{C_2\}$	-	-	-	-	$\{\sigma_v\}$	-	$\{\sigma'_v\}$	
	$\tilde{\mathcal{G}}^{2c}(D_{3h})$	$\{E\}$	-	$\{2C_3\}$	-	$\{3C_2\}$	-	-	$\{2S_3\}$	-	$\{\sigma_h\}$	-	$\{3\sigma_v\}$	
	χ^{2c}	2	0	2	0	2	0	0	2	0	2	0	2	
3f	$\chi_\phi^{\Gamma_4}(p_z)$	2	0	2(-1)	0	-2	0	0	-2(1)	0	-2	0	2	
	$\chi_\phi^{\Gamma_5}(d_{yz,zx})$	4	0	-2 (1)	0	0	0	0	2(-1)	0	-4	0	0	
	$\chi_\phi^{\Gamma_1}(s)$	2	0	2(-1)	0	2	0	0	2(-1)	0	2	0	2	
	$\chi_\phi^{\Gamma_6}(p_{x,y})$	4	0	-2(1)	0	0	0	0	-2(1)	0	4	0	0	
	$\chi_\phi^{\Gamma_7}(s)$	4	0	2(-1)	0	0	0	0	$2\sqrt{3}(-\sqrt{3})$	0	0	0	0	
	$\chi_\phi^{\Gamma_8}(p_z)$	4	0	2(-1)	0	0	0	0	$-2\sqrt{3}(\sqrt{3})$	0	0	0	0	
	$\chi_\phi^{\Gamma_9}$	4	0	-4(2)	0	0	0	0	0	0	0	0	0	
	$\tilde{\mathcal{G}}^{3f}(D_{2h})$	$\{E\}$	-	-	$\{C_2\}$	$\{C'_2\}$	$\{C''_2\}$	$\{i\}$	-	-	$\{\sigma_v\}$	$\{\sigma'_v\}$	$\{\sigma''_v\}$	
	χ^{3f}	3	0	0	3	1	1	3	0	0	3	1	1	
1a	$\chi_\phi^{\Gamma_1^+}(sp_2^+)$	3	0	0	3(-1)	1	1(1)	3(-1)	0	0	3	1(1)	1	
	$\chi_\phi^{\Gamma_2^-}(sp_2^-)$	3	0	0	-3(1)	1	-1(-1)	-3(1)	0	0	3	-1(-1)	1	
	$\chi_\phi^{\Gamma_4^+}$	3	0	0	-3(1)	-1	1(1)	3(-1)	0	0	-3	-1(-1)	1	
	$\chi_\phi^{\Gamma_3^-}$	3	0	0	3(-1)	-1	-1(-1)	-3(1)	0	0	-3	1(1)	1	
	$\chi_\phi^{\Gamma_5^+}$	6	0	0	0	0	0	6(-2)	0	0	0	0	0	
	$\chi_\phi^{\Gamma_5^-}$	6	0	0	0	0	0	-6(2)	0	0	0	0	0	
	$\tilde{\mathcal{G}}^{1a}(D_{6h})$	$\{E\}$	$\{2C_6\}$	$\{2C_3\}$	$\{C_2\}$	$\{3C'_2\}$	$\{3C''_2\}$	$\{i\}$	$\{2S_3\}$	$\{2S_6\}$	$\{\sigma_h\}$	$\{\sigma'_v\}$	$\{\sigma''_v\}$	
1a	$\Gamma_7^+(s)$	2	$\sqrt{3}$	1	0	0	0	2	$\sqrt{3}$	1	0	0	0	
	$\Gamma_8^+(d)$	2	$-\sqrt{3}$	1	0	0	0	2	$-\sqrt{3}$	1	0	0	0	
	$\Gamma_9^+(d)$	2	0	-2	0	0	0	2	0	-2	0	0	0	
	$\Gamma_7^-(p)$	2	$\sqrt{3}$	1	0	0	0	-2	$-\sqrt{3}$	-1	0	0	0	
	$\Gamma_8^-(f)$	2	$-\sqrt{3}$	1	0	0	0	-2	$\sqrt{3}$	-1	0	0	0	
	$\Gamma_9^-(p)$	2	0	-2	0	0	0	-2	0	2	0	0	0	

TABLE II. Decomposition of band representations induced from Wannier orbitals centred on Wyckoff position 2c and 3f of space group 191 on restriction to \mathcal{G}^k at high symmetry point in the Brillouin zone in terms of irreps of \mathcal{G}^k induced from that of $\tilde{\mathcal{G}}^k$.

Wyckoff Position	Orbital	$\Gamma(D_{6h})$	$T(C_{2v})$	$K(D_{3h})$	$T'(C_{2v})$	$M(D_{2h})$	$\Sigma(C_{2v})$
1a	$\Gamma_7^+(s)$	Γ_7^+	T_5	K_7	T'_5	M_5^+	Σ_5
	$\Gamma_8^+(d)$	Γ_8^+	T_5	K_8	T'_5	M_5^+	Σ_5
	$\Gamma_9^+(d)$	Γ_9^+	T_5	K_9	T'_5	M_5^+	Σ_5
	$\Gamma_7^-(p)$	Γ_7^-	T_5	K_8	T'_5	M_5^-	Σ_5
	$\Gamma_8^-(f)$	Γ_8^-	T_5	K_7	T'_5	M_5^-	Σ_5
	$\Gamma_9^-(p)$	Γ_9^-	T_5	K_9	T'_5	M_5^-	Σ_5
2c	$\Gamma_4(p_z)$	$\Gamma_4^+ \oplus \Gamma_2^-$	$T_3 \oplus T_4$	K_5	$T'_3 \oplus T'_4$	$M_4^+ \oplus M_3^-$	$2\Sigma_2$
	$\Gamma_5(d_{yz,zx})$	$\Gamma_5^+ \oplus \Gamma_6^-$	$2T_3 \oplus 2T_4$	$K_3 \oplus K_4 \oplus K_5$	$2T'_3 \oplus 2T'_4$	$M_2^+ \oplus M_4^+ \oplus M_1^- \oplus M_3^-$	$2\Sigma_2 \oplus 2\Sigma_3$
	$\Gamma_1(s)$	$\Gamma_1^+ \oplus \Gamma_3^-$	$T_1 \oplus T_2$	K_6	$T'_1 \oplus T'_2$	$M_1^+ \oplus M_2^-$	$2\Sigma_1$
	$\Gamma_6(p_{x,y})$	$\Gamma_6^+ \oplus \Gamma_5^-$	$2T_1 \oplus 2T_2$	$K_1 \oplus K_2 \oplus K_6$	$2T'_1 \oplus 2T'_2$	$M_1^+ \oplus M_3^+ \oplus M_2^- \oplus M_4^-$	$2\Sigma_1 \oplus 2\Sigma_4$
	$\Gamma_7(s)$	$\Gamma_7^+ \oplus \Gamma_8^-$	$2T_5$	$K_8 \oplus K_9$	$2T'_5$	$M_5^+ \oplus M_5^-$	$2\Sigma_5$
	$\Gamma_8(p_z)$	$\Gamma_8^+ \oplus \Gamma_7^-$	$2T_5$	$K_7 \oplus K_9$	$2T'_5$	$M_5^+ \oplus M_5^-$	$2\Sigma_5$
	Γ_9	$\Gamma_9^+ \oplus \Gamma_9^-$	$2T_5$	$K_7 \oplus K_8$	$2T'_5$	$M_5^+ \oplus M_5^-$	$2\Sigma_5$
3f	$\Gamma_1^+(sp_2^+)$	$\Gamma_1^+ \oplus \Gamma_6^+$	$2T_1 \oplus T_2$	$K_1 \oplus K_6$	$2T'_1 \oplus T'_2$	$M_1^+ \oplus M_2^- \oplus M_4^-$	$2\Sigma_1 \oplus \Sigma_4$
	$\Gamma_2^-(sp_2^-)$	$\Gamma_3^- \oplus \Gamma_5^-$	$T_1 \oplus 2T_2$	$K_2 \oplus K_6$	$T'_1 \oplus 2T'_2$	$M_1^+ \oplus M_3^+ \oplus M_2^-$	$2\Sigma_1 \oplus \Sigma_4$
	$\Gamma_4^+(pd_2^+)$	$\Gamma_4^+ \oplus \Gamma_5^+$	$2T_3 \oplus T_4$	$K_3 \oplus K_5$	$2T'_3 \oplus T'_4$	$M_4^+ \oplus M_1^- \oplus M_3^-$	$2\Sigma_2 \oplus \Sigma_3$
	$\Gamma_3^-(pd_2^-)$	$\Gamma_2^- \oplus \Gamma_6^-$	$T_3 \oplus 2T_4$	$K_4 \oplus K_5$	$T'_3 \oplus 2T'_4$	$M_2^+ \oplus M_4^+ \oplus M_3^-$	$2\Sigma_2 \oplus \Sigma_3$
	Γ_5^+	$\Gamma_7^+ \oplus \Gamma_8^+ \oplus \Gamma_9^+$	$3T_5$	$K_7 \oplus K_8 \oplus K_9$	$3T'_5$	$M_5^+ \oplus 2M_5^-$	$3\Sigma_5$
	Γ_5^-	$\Gamma_7^- \oplus \Gamma_8^- \oplus \Gamma_9^-$	$3T_5$	$K_7 \oplus K_8 \oplus K_9$	$3T'_5$	$2M_5^+ \oplus M_5^-$	$3\Sigma_5$

operations affects characters at HSPs for Wyckoff position 3f.

In evaluating the character of BR upon restriction to \mathcal{G}^k , the TB & Zak basis return the same value. In both cases, the term $\exp[i\mathbf{g}_R \cdot \boldsymbol{\tau}_\alpha]$ is significant at HSPs where $\mathbf{g}_R \neq \mathbf{0}$. The decomposition shown here differs from BANDREP of the Bilbao Crystallographic server²³.

V. BAND CONNECTIVITY OF EBR AND ITS ATOMIC LIMIT, GRAPHENE

Band connectivity is an essential tool in discussing topological properties of electronic band. The nodes in band connectivity (connectivity chord) are the unitary irreps of \mathcal{G} . These corresponds to the energy eigenstate in the crystal and indexed by $\kappa = \mathbf{k} \in \text{RD}$. The

RD in BZ serves as the domain of the dual of the space group¹⁴ with the the unitary irreps of \mathcal{G} as its element. An EBR may be decomposed in the RD as

$$\Gamma_{G^\tau \uparrow}^{\mathcal{G}} = \int_{\kappa \in \text{Rep dom}} D^\kappa(g) d\kappa + D^\Gamma + D^K + D^M + \dots$$

where the integral part depends on the Born-von Karman group or the size of the crystal. The representation at HSPs such as Γ , K , M ... are sub representations independent of size of the crystal. The unitary irrep on high symmetry lines/planes in the RD or a general \mathbf{k} point are fixed by their neighbouring HSPs under compatibility relations²⁴. We are interested in the band connectivity of EBRs in the atomic limit and connectivity of physical bands as determined by the representation matrices of Eq.(14) and the symmetry compliant TB model respectively. Given the Frobenius reciprocity theorem, it is suffice to label these nodes (unitary irrep of \mathcal{G}) with the label of irreps of $\tilde{G}^\mathbf{k}$.

Much of the literature had been focused on the compatibility relation and graph theory. The major hurdle in determining the band connectivity of EBR in the atomic limit is to link HSPs which are *not* immediate neighbours to each other. The analytical form of BR in Eq.(14) allows the hurdle to be overcome.

The tools available to identify EBR connectivity are: 1) decomposition of BR at HSPs assuming absence of accidental degeneracy, 2) compatibility relation/graph theory⁹, and 3) projection operators one is able to construct to establish connectivity between HSPs which are *not* immediate neighbours. We will see the methodology of compatibility relation/graph theory is imbedded and improved upon by projection operator technique. Section IV described the decomposition of an isolated EBR limiting the possible irreps of \mathcal{G} occurring at any wave vector $\mathbf{k} \in \text{RD}$. The following address the use of two remaining tools.

A. Compatibility relations

Compatibility relations links the symmetry of an eigenstate at HSP to that of its immediate neighbours of lower symmetry. This is the consequence of the group/subgroup relations that exist between the little co-group of \mathbf{k} ($\tilde{G}^\mathbf{k}$) at HSP and its lower symmetry *neighbours*. This has no direct link to band representations but they must be satisfied by a physical band and in an EBR. This helps identification of band connectivity in EBRs under atomic limit part of the way.

TABLE III. Compatibility relations between irreducible representations of \tilde{G}^k at high symmetry points Γ , K , M and its neighbours under $\mathcal{G} = 191$ given the relations of symmetry operations of \tilde{G}^k shown in Tab.I

$T(C_{2v}) \downarrow$	T_1	T_3	$T_3 \oplus T_4$	$T_1 \oplus T_2$	T_4	T_2	$T_1 \oplus T_2$	$T_3 \oplus T_4$	T_5	T_5	T_5
$\Gamma(D_{6h})$	Γ_1^+	Γ_4^+	Γ_5^+	Γ_6^+	Γ_2^-	Γ_3^-	Γ_5^-	Γ_6^-	Γ_7^\pm	Γ_8^\pm	Γ_9^\pm
$\Sigma(C_{2v}) \downarrow$	Σ_1	Σ_2	$\Sigma_2 \oplus \Sigma_3$	$\Sigma_1 \oplus \Sigma_4$	Σ_2	Σ_1	$\Sigma_1 \oplus \Sigma_4$	$\Sigma_2 \oplus \Sigma_3$	Σ_5	Σ_5	Σ_5
$T \& T'(C_{2v}) \downarrow$	T_1	T_2	T_3	T_4	$T_3 \oplus T_4$	$T_1 \oplus T_2$	T_5	T_5	T_5	T_5	T_5
$K(D_{3h})$	K_1	K_2	K_3	K_4	K_5	K_6	K_7	K_8	K_9		
$T'(C_{2v}) \downarrow$	T_1	T_4	T_2	T_3	T_5	T_3	T_2	T_4	T_1	T_5	
$M(D_{2h})$	M_1^+	M_2^+	M_3^+	M_4^+	M_5^+	M_1^-	M_2^-	M_3^-	M_4^-	M_5^-	
$\Sigma(C_{2v}) \downarrow$	Σ_1	Σ_3	Σ_4	Σ_2	Σ_5	Σ_3	Σ_1	Σ_2	Σ_4	Σ_5	

For honeycomb lattice with space group $\mathcal{G} = 191$, the real and reciprocal space presentation is the same as shown in Fig.1. The operations of \tilde{G}^k at different HSPs are identified in Tab.I. The characters of the irreps of \tilde{G}^k are readily available and the compatibility relation of irreducible representation of \tilde{G}^k at HSPs, such as Γ with its lower symmetry neighbours can be established using the relations between \tilde{G}^k shown in Tab.I and relevant character table of point groups³⁰. For all the relevant irreps that occur in the decomposition at Γ , T , K , T' , M and Σ , the compatibility relations are listed in Tab.III. It is important to

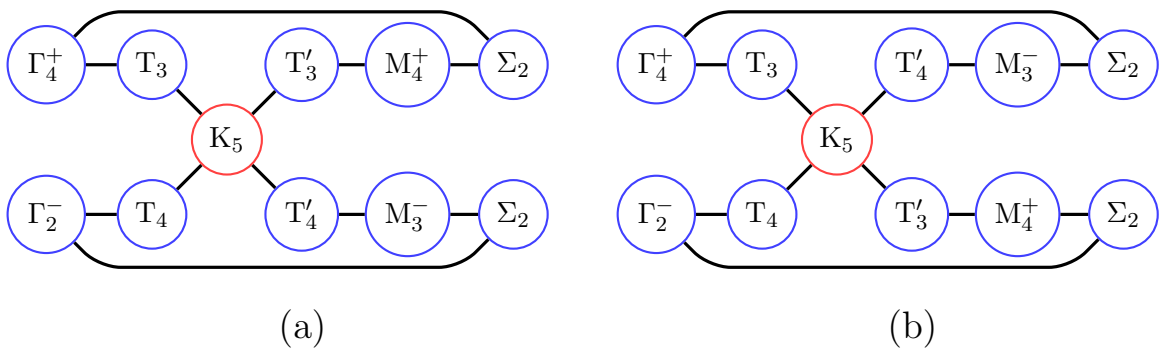


FIG. 2. Connected graph relating to the band structure, described by the spinless band representation induced from p_z orbital on Wyckoff position 2c of honeycomb lattice, based on compatibility relations and graph theory. The degeneracy that existed at K ensures the system is in semi-metal phase for half filling of the band.

recognise that such compatibility relation only exist between high symmetry point and its lower symmetry neighbours. No relation between the Γ , K or M points is determined by the compatibility relations as they are separated in k -space by T , T' and Σ .

It is possible to discuss symmetry allowed band connectivity using combination of compatibility relations, decomposition of band representations and graph theory³. For example, the band representation from p_z orbital without spin on Wyckoff position 2c can generate connected HSPs as shown in Fig.2. Only one connected component exist. There are two possible configurations permitted by the combination of compatibility relations, decomposition of BR and graph theory. The ambiguity between the two configurations remain under these considerations. Both lead to semi-metal phase when the band is half filled. The use of analytical form of band representation allows these ambiguity to be resolved.

B. Connectivity in EBR and its atomic limit

Given a band representation (space group \mathcal{G} , Wyckoff position τ_α , and Wannier function $\phi_{\mu,i}^{\tau_\alpha}$), its transformation properties is determined by Eq.(14) and Eq.(13). We recall that the basis of these representations are Bloch sums constructed from $\phi_{\mu,i}^{\tau_\alpha}(\mathbf{t} - (\mathbf{t}_\ell + \tau_\alpha))$ indexed by the Wyckoff position label τ_α and irrep label μ of the site symmetry group. It is free to choose linear combination of these as basis. The issue of interest here is band connectivity and what happens in absence of any interaction (atomic limit). In the atomic limit, no inter-site interaction is allowed. Therefore there is no \mathbf{k} dependent mixing of basis. The underlying link between the nodes is the basis of nodes in EBR which ‘propagate’ the transformation properties in the RD. The possibility of a link between any two nodes can be easily obtained using projection operator one is able to construct using (14). The connectivity established via the projection operator does not confer any energetic order.

Utilising the Frobenius reciprocity theorem, we work with \mathcal{G}^k , its irreps and the subduced EBR. The irreps of \mathcal{G}^k is given by Eq.(23) and labelled by the p . A node may correspond to multi-dimensional irrep of \mathcal{G}^k and links are connected to terminals labelled by its indices. The subduced EBR at \mathbf{k} is obtained from Eq.(14) by setting $\mathbf{k}' = \mathbf{k}$ and it is labelled by τ and μ .

$$\Gamma_{\mathcal{G}(\tilde{\mathcal{G}}_\mu^k) \downarrow}^{\mathcal{G}^k}(\{R|\mathbf{v} + \mathbf{t}\})_{\tau'_\alpha, i'; \tau_\alpha, i} = \exp\{i[\mathbf{k} \cdot (\tau'_\alpha - \tau_\alpha) + \mathbf{g}_R \cdot \tau_{\alpha'}]\} \exp\{-iR\mathbf{k} \cdot (\mathbf{v} + \mathbf{t})\} \times D^\tau(R)_{\tau'_\alpha, \tau_\alpha} \otimes D^\mu(R_{\leftarrow}^\tau(R, R_{\alpha'}^\tau))_{i'i} \quad \{R|\mathbf{v} + \mathbf{t}\} \in \mathcal{G}^k. \quad (27)$$

The projection operator, identified by the node (\mathbf{k}, p) , can then be constructed in the normal way.

$$\hat{\mathcal{P}}_{i,j}^{\mathbf{k},p} = \frac{1}{|\mathcal{G}^{\mathbf{k}}|} \sum_{g \in \mathcal{G}^{\mathbf{k}}} \Gamma_{\tilde{G}_p^{\uparrow}}^{g^{\mathbf{k}}}(g)_{i,j}^* \Gamma_{\mathcal{G}(\tilde{G}_p^{\uparrow})\downarrow}^{g^{\mathbf{k}}}(g)_{\tau'_\alpha, i'; \tau_\alpha, i} \quad (28)$$

The summation over the translation sub-group is factored out. We only need to sum over the coset representatives in the decomposition of $\mathcal{G}^{\mathbf{k}}$ as left cosets of \mathcal{T} or simply elements of $\tilde{G}^{\mathbf{k}}$ with change of normalisation from $|\mathcal{G}^{\mathbf{k}}|$ to $|\tilde{G}^{\mathbf{k}}|$.

How do we see link between two nodes which are not immediate neighbours in the framework of projection operators. Clearly, a potential link exist if some linear combination of basis give rise to a node at (Γ, p) (here Γ specify $\mathbf{k} \in \text{RD}$ and p specify the irrep of \tilde{G}^Γ) also can contribute towards node at (M, q) and vice versa. Then there exist

$$\hat{\mathcal{P}}_{i,i}^{(M,q)} \hat{\mathcal{P}}_{j,j}^{(\Gamma,p)} \neq \text{Null} \quad \& \quad \hat{\mathcal{P}}_{j,j}^{(\Gamma,p)} \hat{\mathcal{P}}_{i,i}^{(M,q)} \neq \text{Null} \quad (29)$$

for some combination of indices i, j of irrep p and q labelling the terminals of the nodes. The two relations are the transpose of the projection operator matrix relation. The link is not necessarily exclusive between two nodes. When

$$\hat{\mathcal{P}}_{i,i}^{(M,q)} \hat{\mathcal{P}}_{j,j}^{(\Gamma,p)} = \hat{\mathcal{P}}_{j,j}^{(\Gamma,p)} \neq \text{NULL} \quad (30)$$

The link only connect two nodes exclusively. Such link is called a simple link and exist for definite in physical band connectivity. When a link is associated with more than two nodes, such link is called complex. For the link to exist between (Γ, p) and (M, q) , compatibility relation must also be satisfied via their lower symmetry intermediate. It is, of course, guaranteed by symmetry and the representation matrices. Two nodes that are not linked directly may still be linked via nodes at other HSPs. For example, one may have

$$\hat{\mathcal{P}}_{i,i}^{(\Gamma,q)} \hat{\mathcal{P}}_{j,j}^{(\Gamma,p)} = \text{NULL} \quad \& \quad \hat{\mathcal{P}}_{i,i}^{(\Gamma,q)} \hat{\mathcal{P}}_{l,m}^{(M,r)} \hat{\mathcal{P}}_{j,j}^{(\Gamma,p)} \neq \text{NULL}.$$

If any two nodes from an EBR are on separate disconnected component bands *under atomic limit*, then there should be no link of any kind between the two nodes.

To obtain physical band connectivity of an EBR, one can go through all the nodes identified by the decomposition of an EBR and establish all the relevant links permitted by the projection operator scheme which automatically satisfy the compatibility relations. To find out what band connectivity can occur in nature, the complex links need to be resolved

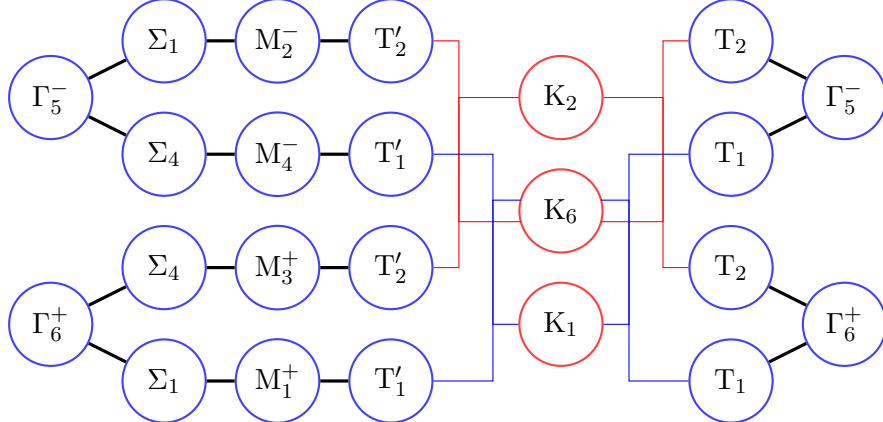


FIG. 3. Link diagram of EBR from spin-less $p_{x,y}$ orbital on Wyckoff position 2c of honeycomb lattice in atomic limit. Simple links are shown in thick lines and complex links are shown in thin lines involving more than 2 nodes/terminals. All links to nodes at K are complex.

into simple links because a link can only join two nodes/terminals from dimensionality consideration. This lead to potentially multiple configurations. In particular, some of these configurations permitted under compatibility relations alone can contain disconnected component bands. The following argument shows that such configuration is not permitted by an EBR *under atomic limit*, thus resolving the debate on fully connected nature of EBR. An EBR is always *connected in the atomic limit* and a disconnected EBR connectivity *does not have an atomic limit*.

We are considering EBR which cannot be decomposed into composite of other EBRs by definition. Let's assume an EBR contains two disconnected component bands and nodes (A, p_1) , (A, p_2) , and (B, q_1) , (B, q_2) . The component bands are indexed by suffix 1 and 2. As an EBR, the basis is complete and state at any \mathbf{k} can be expressed as linear combination of Bloch sum basis that give rise to nodes at A or B in the RD. The transformation properties are fixed by Eq.(14). Under the atomic limit, there is no inter-site interaction or mixing of basis. Thus each of the nodes (B, q_1) in the component band 1 must be expressible as linear combination of Bloch sums which give rise to (A, p_1) to the exclusion of (A, p_2) . This requires the BR expressible as direct sums of two BRs and contradicting the assumption of EBR under atomic limit. Hence an EBR must be fully connected in the atomic limit. We illustrate how this may be tested using projection operator in an example below.

The connectivity of EBR on Wyckoff position with multiplicity of 1 (per primitive cell)

and those from Wannier function of dimension 1 on Wyckoff position with multiplicity of 2 are simply connected. Returning to EBR induced from p_z orbital on Wyckoff position 2c of a honeycomb lattice, one can easily verify the existence of simple link between Γ_4^+ and M_4^+ but absence of link between Γ_4^+ and M_3^- . Therefore, Fig.2a is the correct connectivity and Fig.2b is excluded from allowed band connectivity of the EBR.

Connectivity of EBR in more complex situation may involve complex links and encounter multiple configuration of physical connectivity. Under compatibility relations alone, the permitted physical connectivity may not be simply connected. Here we take the example of EBR induced from $p_{x,y}$ orbital (Γ_6 of G^7) on Wyckoff position 2c of honeycomb lattice ($\mathcal{G} = 191$). We show that this EBR have multiple configurations of physical connectivity but its atomic limit remains connected. The decomposition of the EBR at HSPs can be read from Tab.II. The links between nodes at Γ and M are all simple. Links involving nodes at K points are all complex and each terminal on nodes at K is allowed to connect to multiple terminals/nodes at other HSPs. Links in this EBR under atomic limit are established and shown in Fig.3.

From the links of EBR under atomic limit, possible conforming physical band connectivity are generated by replacing the complex links with permitted simple links. A link in physical system can only join two nodes/terminals in consideration of dimensionality. This leads to a number of possible physical band connectivity which may not all be permitted in the atomic limit. Some are shown in Fig.4. Utilising symmetry compliant Hamiltonian described in Sec.III and appendix B-C, physical connectivity shown in (a) and (b) of Fig.4 are realised as shown in Fig.5. Configuration (a) of the connectivity is produced with nearest neighbour interaction only and TB parameter $t_{\Gamma_6, \Gamma_6}^{FNN:A} = -1$ and $t_{\Gamma_6, \Gamma_6}^{FNN:B} = -4$. The resulting dispersion is shown in Fig.5a. Configuration (b) is produced by further inclusion of a second nearest neighbour interaction term with parameter $t_{\Gamma_6, \Gamma_6}^{SNN:D}$. This is a symmetry permitted second nearest neighbour interaction not considered under the Slater Koster formulation. Changing this parameter from -1 to -3, a gap is developed in the $K\Gamma$ direction, but the K_6 nodes remain connected to the Γ_6^+ and Γ_5^- nodes in the $KM\Gamma$ direction. The energy dispersion calculated is shown in Fig.5b. As explained in great detail in the supplement of Ref.[21], a gapped state is produced with a limited range of parameters²⁵. It is reproduced with $t_{\Gamma_6, \Gamma_6}^{FNN:A} = 0.9$ and $t_{\Gamma_6, \Gamma_6}^{FNN:B} = 0.1$ and $|t_{\Gamma_6, \Gamma_6}^{SNN:D}| > 0.04$. This correspond to the disconnected configuration (c). However, is configuration (c) permitted by the EBR under atomic limit? For the EBR

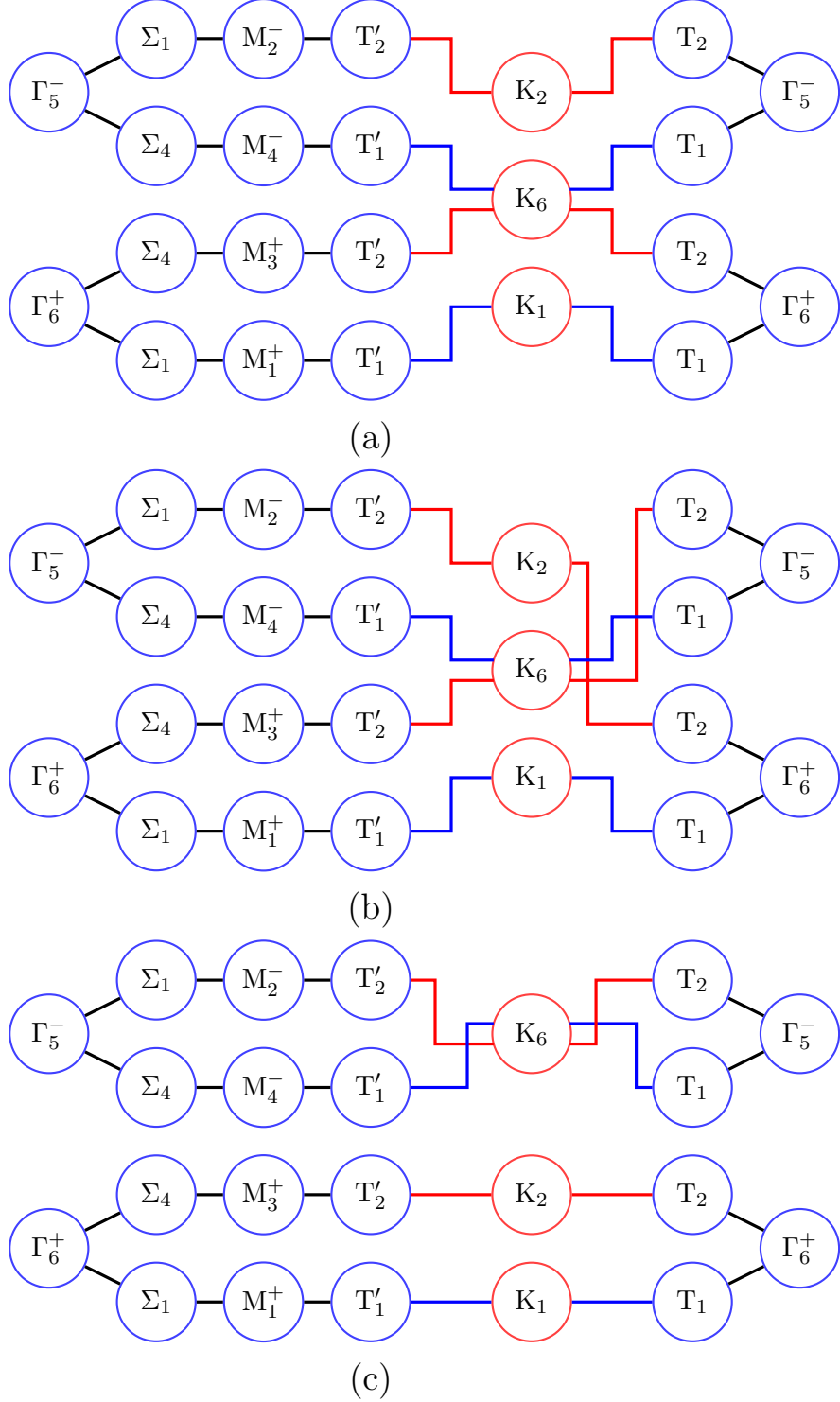


FIG. 4. Band connectivity of possible physical band from spin-less $p_{x,y}$ orbital on Wyckoff position 2c of honeycomb based on compatibility. There are other configurations not displayed here. (c) differs from (a) and (b) in topology since it contains two disconnected components. However, it is excluded by projection operators.

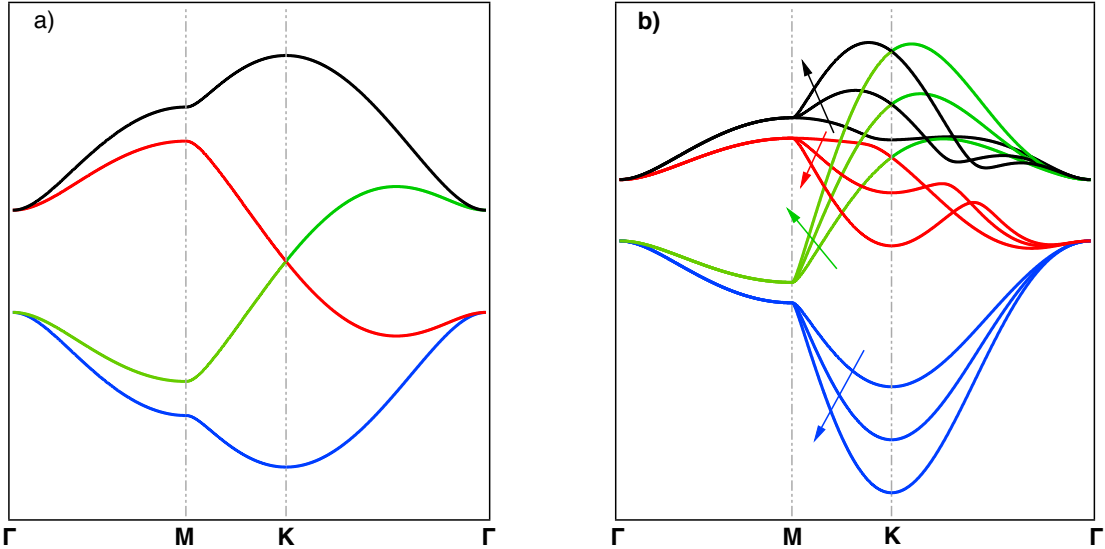


FIG. 5. Energy dispersion of EBR induced from p_{xy} orbital on Wyckoff position 2c of honeycomb lattice. a) nearest neighbour interaction only with $t_{\Gamma_6, \Gamma_6}^{FNN:A} = -1$ and $t_{\Gamma_6, \Gamma_6}^{FNN:B} = -4$, b) addition of second nearest neighbour interaction with $t_{\Gamma_6, \Gamma_6}^{SNN:D} = -1, -2, -3$.

in atomic limit to be disconnected as shown in configuration (c), the states corresponding to node K_6 must be orthogonal (exclude contribution from linear combination of basis which give rise to) to states at node Γ_6^+ . But projection operator

$$\hat{P}_{1,1}^{\Gamma,6+} \hat{P}_{1,1}^{K,6} \neq \text{NULL}.$$

Hence such orthogonality is not permitted by the EBR in the atomic limit. This means configuration (c), the topologically disconnected physical connectivity, does not have an atomic limit. The EBR remains *connected in the atomic limit* and the topological order of the atomic limit of this EBR is protected by symmetry.

The methodology developed here goes directly from decomposition of EBR to connectivity of the EBR in one step. The compatibility relation/graph theory is built in and enhanced.

C. Graphene as topological insulator as viewed from band connectivity

While it is well known that graphene is a topological insulator, it has not been clearly established from band connectivity perspective under the atomic limit. The tools afforded here by the analytical BR allows an insight how this arise in comparison to others approach

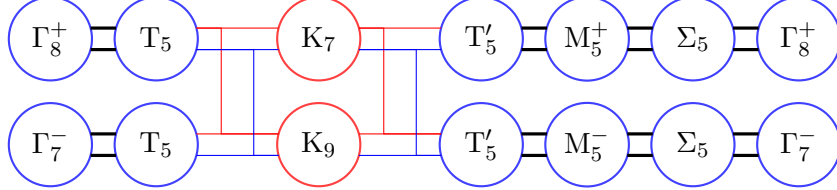


FIG. 6. Link diagram of EBR induced from spinful p_z orbital on Wyckoff position 2c in atomic limit.

such as band inversion.

We need to establish connectivity of EBR from spin-ful p_z orbital ($\mu = \Gamma_8$ of $\tilde{G}\tau = D_{3h}$) in the asymptotic limit of large lattice parameter. The decomposition of this EBR is already shown in Tab.II. Using the projection operator technique outline above, the link diagram of this EBR is obtained and shown in Fig.6. Links to nodes at K are again complex. We need to examine physical band connectivity, with some possible configurations shown in Fig.7. The band connectivity shown in configuration a) or b) had been the basis for explaining that graphene (Rice-Mele model) is a fragile topological insulator as the disconnected band connectivity does not have an atomic limit. Indeed Ref[20] proposed a mechanism of topological phase transition from TI to classical insulator though the work is based on $\mathcal{G} = 183$ with possible Rashba term. In the context of $\mathcal{G} = 191$, all of the component bands in configuration a) or b) could not be described by the EBR induced from Wyckoff position 1a. They remain topological. The mechanism of switching energetic order at Γ would not have induced a change of topological order in terms of connectivity, at least in absence of Rashba term since both (a) and (b) are gapped.

An alternative view would make graphene a strong topological insulator. Consider the band connectivity shown in configuration (c). The topological nature of the band arise when interactions are restored in real crystals and inter-site spin dependent interaction lifts the degeneracy between K_7 and K_9 . The creation of a bulk gap at K separate the *bulk* dispersion into two physical bands. This is easily verified by symmetry compliant TB model. However, it does not alter the band connectivity shown in Fig.8. As there is a bulk gap at K, the only way to sustain the connections between nodes at K and Γ across the gap is the edge states with the corresponding bulk boundary correspondence. Essentially, the connected nature of the two bulk gapped bands can not be removed by the homeomorphic transformation in the manifold introduced by TB parameters.

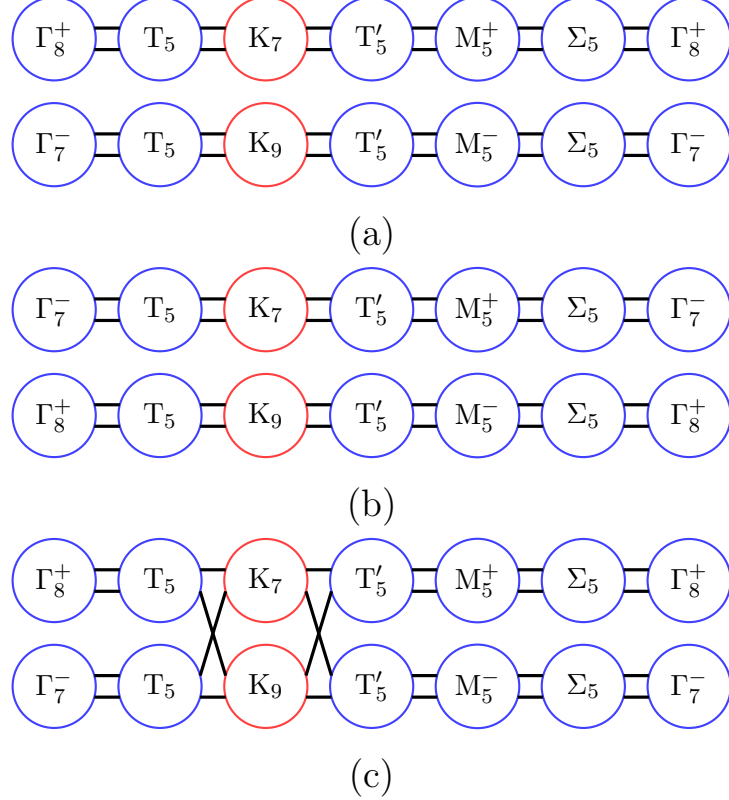


FIG. 7. Possible physical band connectivity of EBR induced from spin-ful p_z orbital on Wyckoff position 2c. a) and b) are disconnected and do not have an atomic limit. c) is connected and permitted by symmetry.

Which of the two configuration in Fig.8 occurs in nature depends on the sign of inter-site spin dependent interaction. If one subscribe to the idea of spin-dependent interaction via remote d-levels²⁶, then it will depends on the energetic order of the remote d-levels (Γ_7 and Γ_9 of the site symmetry group). If one subscribe to the effective Hamiltonian with second nearest neighbour interaction²⁷ as shown in Section III and appendix B-C, then it is simply the sign of the TB parameter $t_{\Gamma_8, \Gamma_8}^{SNN:B}$ associated with the symmetry permitted second nearest neighbour interaction. The resulting connectivities shown in Fig.8 are no longer equivalent.

Is there any supporting argument for a ‘super link’ across an energy gap? Consider the EBR induced from spin-less and spin-ful 1s (Γ_1^+ and Γ_5^+ of D_{2h}) orbital on Wyckoff position 3f. As a spin-less EBR, it has a connectivity indicated in Fig.9b which is connected and has an atomic limit. Introducing the spin, and *if one believe that the corresponding connectedness does not change*, then we are faced with the same required ‘super link’ across the gap as

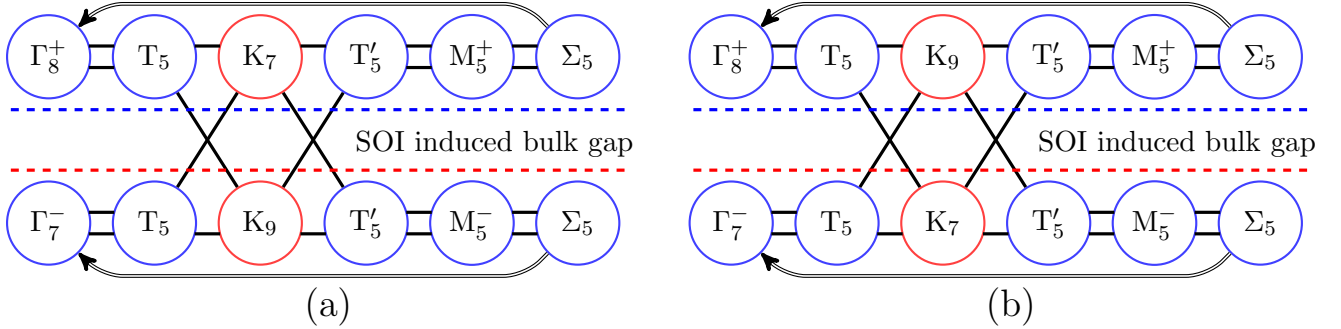


FIG. 8. Band connectivity of EBR induced from spin-ful p_z orbital on Wyckoff position 2c. The irreps K_7 and K_9 are degenerate in the asymptotic limit as all interactions, including inter-site spin-orbit interactions are set to zero.

$K_6 \rightarrow K_8 \oplus K_9$. Such link does not show in TB calculations. The same argument can be made on p_z orbital itself on Wyckoff position 2c through comparison of spin-less and spin-ful cases. The spin-less case has only one possible band connectivity with atomic limit shown in Fig.2a. Including the spin, the gap occurs as $K_5 \rightarrow K_7 \oplus K_9$. If the atomic limit still exist after the introduction of spin, then we expect a connectivity with atomic limit such as the one shown in Fig.7c.

It is important to recognise that the proposed EBR connectivity remains connected via the edge state, at least in this case. The topological nature of the bands does not come from band inversion, but from the connectedness of the EBR that exist across the bulk gap. This proposal of graphene as strong TI is very different from the band connectivity offered in Fig.3a of Ref.[7], though the space group used there is $\mathcal{G} = 183$. Because of the topological property arise from connected EBR at half filling and existence of bulk gap, the bulk edge correspondence can not be removed by inverting the energetic order of nodes at Γ point as proposed in Ref.[20]. It is also interesting to note the difference in connectivity in the example of EBR induced from spin-less p_{xy} and that of spin-ful p_z orbitals. The former can be seen in full dispersion calculated by TB model but the latter is across the gap hidden in edge state with bulk boundary correspondence.

D. Equivalent BR, classic insulator band, and symmetry indicator method

An important point one learns from the last sub-section is that a node in band connectivity can have linkage across the energy gap in physical bands via bulk-boundary correspondence as in the case of graphene. Such linkage is guaranteed by the band connectivity with atomic limit. If one accepts that an EBR connectivity with atomic limit is always connected, what constitute a classical insulator, equivalence of band representation and band inversion can be clarified. Here we examine the sp_2 hybridised backbone of graphene as an example

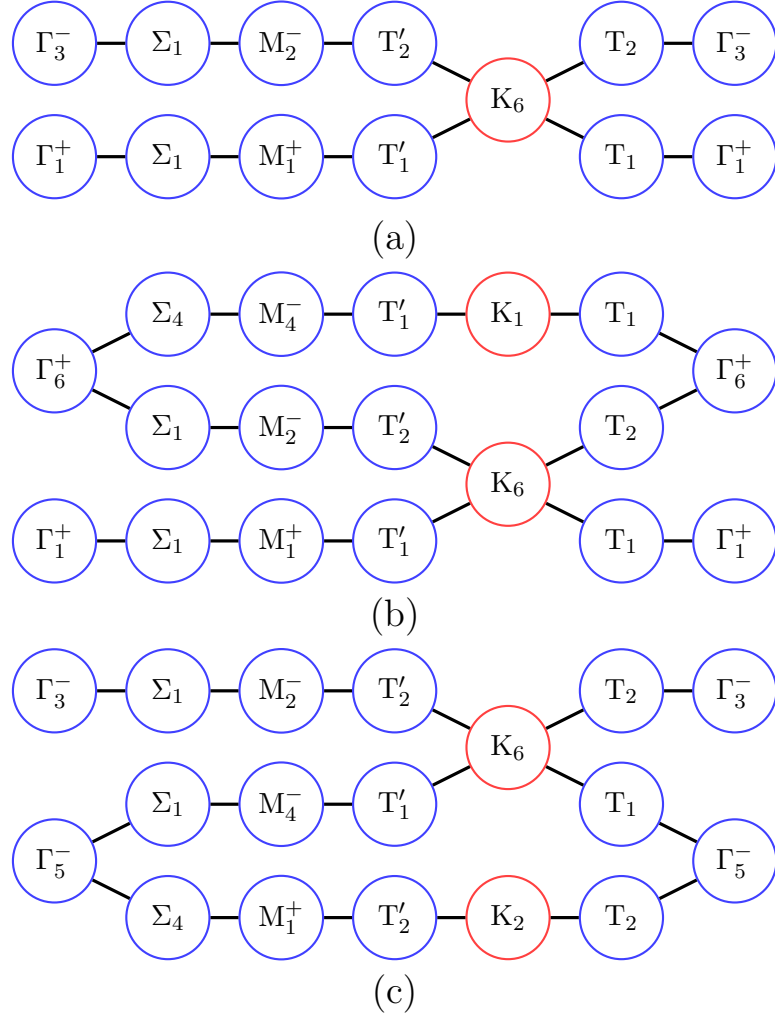


FIG. 9. Band connectivity of EBR from spin-less orbitals on honeycomb lattice ($G = 191$). (a) s (Γ_1) orbital on Wyckoff position 2c under atomic limit; physical band connectivity permitted by EBR form (b) s (Γ_1^+) orbital on Wyckoff position 3f, and (c) p_y (Γ_2^-) orbital on Wyckoff position 3f.

of a classical insulator bands. The band connectivity of p_{xy} orbitals are already discussed. The band connectivity of s orbital on Wyckoff position 2c contains only simple link and is shown in Fig.9(a). The band connectivity of EBR induced from s (Γ_1^+ of D_{2h}) orbital on Wyckoff position 3f, and p_y (Γ_2^- of D_{2h}) orbital on Wyckoff position 3f involves complex links connected to nodes at K. Physical band connectivity with atomic limit permitted by the EBR are shown in Fig.9 (b) and (c). Using the symmetry compliant TB Hamiltonian and well accepted Slater Koster parameter, insulator phase are obtained from TB basis from s and p_{xy} orbitals. Extracted band connectivity from TB calculation is shown in Fig.10 and clearly shows a copy of sum of connectivity of EBRs induced from Γ_1^+ and Γ_2^- orbitals on Wyckoff position 3f. The breaking of linkages present in EBRs induced from s and p_{xy} orbital on Wyckoff position 2c (between nodes in valence band (Γ_1^+ and Γ_6^+) and conduction band (Γ_2^- and Γ_5^-)) at Γ via nodes at K (K_6) is achieved by dynamic interaction of s and p_{xy} orbitals. The two linkage that existed in individual EBRs “annihilated” each other and

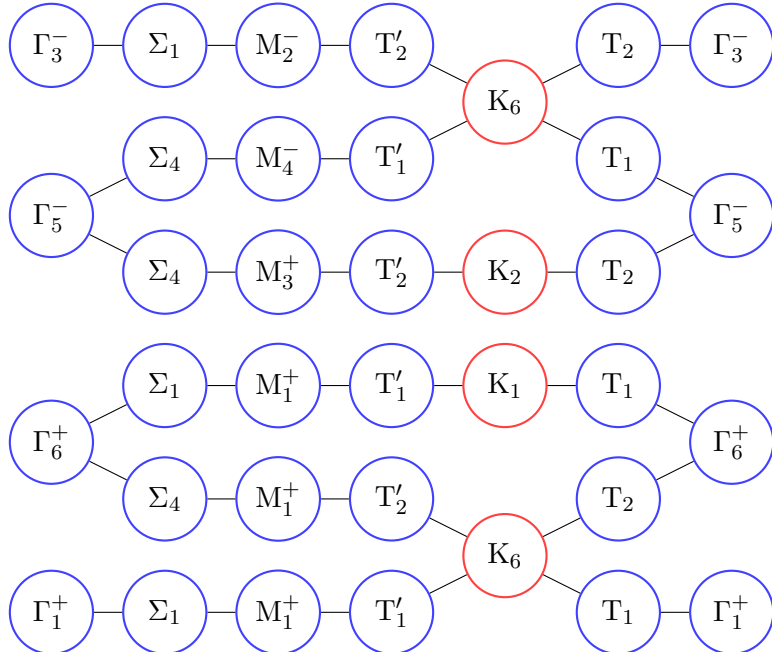


FIG. 10. (Band connectivity extracted from TB calculation with TB basis induced from s and p_{xy} orbitals on Wyckoff position 2c. Typical Slater Koster parameter is used to produce the insulator phase.

produce the band gap and “dynamic” equivalence below:

$$\Gamma_{\tilde{G}_{\Gamma_1}^{2c}\uparrow}^{\mathcal{G}} \oplus \Gamma_{\tilde{G}_{\Gamma_6}^{2c}\uparrow}^{\mathcal{G}} \equiv \Gamma_{\tilde{G}_{\Gamma_1^+}^{3f}\uparrow}^{\mathcal{G}} \oplus \Gamma_{\tilde{G}_{\Gamma_2^-}^{3f}\uparrow}^{\mathcal{G}}$$

It is important to recognise that such equivalence is “dynamic”, or only exist for certain range of TB parameters. It is not guaranteed by the symmetry.

The example here allows some insight into dynamic equivalence of BRs. An EBR is always connected and closed. There is no exterior connection as the dimensions of subduced irreps of \mathcal{G}^k is always the same at any \mathbf{k} . So for a physical band to be described by a composite of EBRs, it must have the same decomposition at HSPs as the composite EBR. In addition, all the nodes must be “satisfied” internally and no external connection exist. If we examine the sp_2 bands with spin, the valance band would break into three disconnected physical bands but with linkage across mini-gaps within in valance band at K point. Externally, there are no unsatisfied nodes and system remains as classical insulator band under the dynamic equivalence:

$$\Gamma_{\tilde{G}_{\Gamma_7}^{2c}\uparrow}^{\mathcal{G}} \oplus \Gamma_{\tilde{G}_{\Gamma_8}^{2c}\uparrow}^{\mathcal{G}} \oplus \Gamma_{\tilde{G}_{\Gamma_9}^{2c}\uparrow}^{\mathcal{G}} \equiv \Gamma_{\tilde{G}_{\Gamma_5^+}^{3f}\uparrow}^{\mathcal{G}} \oplus \Gamma_{\tilde{G}_{\Gamma_5^-}^{3f}\uparrow}^{\mathcal{G}}$$

Thus the definition of a classic insulator band is one that can be described by composite EBRs with atomic limit under the dynamics of the system. With this, the concept of band inversion, such as those in α -Sn, can lead to topological phase. Here, the inversion is from the sp_3 classic insulator band described by EBR induced form Wannier functions on Wyckoff position c of space group $\mathcal{G} = 227$. With band inversion, the valence band can no-longer be described by the EBR and connection to external node must be present.

This also provide some physical basis of symmetry indicator method. If one accepts that EBRs subject to atomic limit are connected and closed, then the symmetry indicator method is just a manifestation of classical insulator band being described by the composite EBRs subject to the existence of atomic limit. This, of course, is subject to the correct decomposition of EBRs as described in Sec.IV.

VI. SUMMARY

Band representation, proposed in the early 80’s, enabled the recent topological quantum chemistry work. The corrected definition of basis in this manuscript allowes derivation of appropriate transformation matrices for BR. This, in turn, allows the construction of

symmetry compliant Hamiltonian and projection operators. A clearly defined methodology is devised to construct band connectivity, bridging the gap between any two HSPs in wavevector space which cannot be determined by compatibility relationship. Concepts of simple and complex links between nodes are introduced. Realisation of physical band connectivity from linked nodes of EBR under atomic limit decompose complex links into simple links. This explains naturally how a single EBR can lead to different physical band connectivity. Symmetry argument shows any disconnected EBRs do not have an atomic limit. Using symmetry compliant TB Hamiltonian, the transition between different physical connectivity is demonstrated. It maintains that topological order of EBRs in atomic limit are protected by the symmetry. In particular, the crucial spin-ful p_z induced EBR on honeycomb lattice can remain connected via the edge state in bulk boundary correspondence and explains the topological nature of electron dispersion in graphene.

The methodology is solely based on symmetry analysis, staying true to the motto of topological quantum chemistry. The symmetry compliant TB Hamiltonian allows the exploration of any homeomorphic transformation of the dispersion surfaces and extract the connectivity of physical bands where multiple EBRs are used as basis. The full connectivity of EBR under atomic limit now provide a direct physical reason for the symmetry indicator methods based on the correspondence between occupation of full composite EBRs with atomic limit and classical insulator phase.

ACKNOWLEDGMENTS

The author wishes to acknowledge the Department of Physics and Institute of Advanced Studies at Tsinghua University for supporting his sabbatical leave during the 2018/19 academic year. Without their support, this work would not have been possible. The author also wishes to thank Professors Bangfen Zhu, Xi Chen, Zheng Liu, Zhengyu Weng at Tsinghua and Dimitri D Vvedensky at Imperial for guidance and discussions.

Appendix A: Some group theoretical concept on the representation of space group

We need to clarify a number of group theoretical concept on space group \mathcal{G} and its representation. The translation operations form an invariant subgroup \mathcal{T} of the space group. In the left coset decomposition of \mathcal{G} , we have

$$\mathcal{G} = \{R_1|\mathbf{v}_1\}\mathcal{T} + \{R_2|\mathbf{v}_2\}\mathcal{T} + \cdots + \{R_i|\mathbf{v}_i\}\mathcal{T} + \cdots + \{R_h|\mathbf{v}_h\}\mathcal{T}. \quad (\text{A1})$$

The rotational part of the coset representatives R_i form the isogonal point group F which is isomorphic to the quotient group \mathcal{G}/\mathcal{T} . The coset representatives generally do not form a group. But in the case of symmorphic space group where all non-lattice translations $\mathbf{v}_i = \mathbf{0}$, they form the point group F .

A set of equivalent Wyckoff positions with multiplicity m have position vector τ_α in the primitive cell with $\alpha = 1, \dots, m$. They form the orbit of the Wyckoff position in the primitive cell. Each position τ_α may be reached from τ_1 with some space group operation

$$\{R_\alpha^\tau|\mathbf{v}_\alpha^\tau + \mathbf{t}\}\tau_1 = \tau_\alpha \quad (\text{A2})$$

where \mathbf{t} is a lattice translation determined by α . Each of the position has the “site symmetry group” $G^{\tau,\alpha}$ whose members leaves τ_α invariant. $G^{\tau,\alpha}$ forms an invariant subgroup of the space group. These site symmetry groups are conjugate to each other.

$$G^{\tau,\alpha} = \{R_\alpha^\tau|\mathbf{v}_\alpha^\tau + \mathbf{t}\}G^{\tau,1}\{R_\alpha^\tau|\mathbf{v}_\alpha^\tau + \mathbf{t}\}^{-1} \quad (\text{A3})$$

Its rotational part (co-group of τ) $\tilde{G}^{\tau,\alpha}$ also form a subgroup of the isogonal point group F of the crystal. $\tilde{G}^{\tau,\alpha}$ is isomorphic to $\tilde{G}^\tau = \tilde{G}^{\tau,1}$ (as per the definition of Wyckoff position). In the left coset decomposition of the isogonal point group F with respect to \tilde{G}^τ , the coset representatives are chosen once and designated as R_α^τ .

$$F = R_1^\tau \tilde{G}^\tau + \cdots + R_\alpha^\tau \tilde{G}^\tau + \cdots + R_m^\tau \tilde{G}^\tau, \quad R_1^\tau = E \quad (\text{A4})$$

where m is the multiplicity of the Wyckoff position. There is a one to one correspondence of R_α^τ in Eq.(A2) and Eq.(A4). Hence

$$\tilde{G}^{\tau,\alpha} = R_\alpha^\tau \tilde{G}^\tau R_\alpha^{\tau-1} \quad (\text{A5})$$

Given $R \in F$, and $R_\beta^\tau, RR_\beta^\tau \in F$. Therefore RR_β^τ must be in some unique coset with representative R_α^τ and

$$R_\alpha^\tau R_\rightarrow^\tau(R, R_\beta^\tau) = RR_\beta^\tau, \quad R_\rightarrow^\tau(R, R_\beta^\tau) \in \tilde{G}^\tau \quad (\text{A6})$$

where R_α^τ and $R_\rightarrow^\tau(R, R_\beta^\tau)$ are uniquely determined by R and R_β^τ . Conversely, we can say that given R and R_α^τ , $R_\leftarrow^\tau(R, R_\alpha^\tau)$ and R_β^τ are uniquely determined in

$$R_\alpha^\tau R_\leftarrow^\tau(R, R_\alpha^\tau) = RR_\beta^\tau, \quad R_\leftarrow^\tau(R, R_\alpha^\tau) \in \tilde{G}^\tau \quad (\text{A7})$$

In forming the irreducible space group representation in the conventional way²², the concept of little co-group of \mathbf{k} : was introduced. $\tilde{G}^\mathbf{k}$ is a subgroup of F , whose action preserves the wave vector such that

$$R\mathbf{k} \equiv \mathbf{k}; \text{ or } R\mathbf{k} = \mathbf{k} + \mathbf{g}_R; \quad R \in \tilde{G}^\mathbf{k} \quad (\text{A8})$$

where \mathbf{g}_R is a reciprocal lattice vector. The isogonal point group F is decomposed as left coset of $\tilde{G}^\mathbf{k}$

$$F = R_1^\mathbf{k} \tilde{G}^\mathbf{k} + \cdots + R_\gamma^\mathbf{k} \tilde{G}^\mathbf{k} + \cdots + R_q^\mathbf{k} \tilde{G}^\mathbf{k}, \quad (\text{A9})$$

where there is a one-to-one correspondence between the coset representatives and the arms of star of \mathbf{k} . The coset representatives are chosen once and designated $R_\gamma^\mathbf{k}$. A space group called the little group of \mathbf{k} : $\mathcal{G}^\mathbf{k}$, whose action on Bloch functions leaves the wave vector invariant is constructed as

$$\mathcal{G}^\mathbf{k} = \{R_{\mathbf{k},1}|\mathbf{v}_1\}\mathcal{T} + \cdots + \{R_{\mathbf{k},\beta}|\mathbf{v}_\beta\}\mathcal{T} + \cdots + \{R_{\mathbf{k},b}|\mathbf{v}_b\}\mathcal{T}, \quad R_{\mathbf{k},\beta} \in \tilde{G}^\mathbf{k} \quad (\text{A10})$$

$\mathcal{G}^\mathbf{k}$ is a subgroup of the space group \mathcal{G} which can be expressed as left coset partition of $G^\mathbf{k}$:

$$\mathcal{G} = \{R_1^\mathbf{k}|\mathbf{v}_1\}\mathcal{G}^\mathbf{k} + \cdots + \{R_\gamma^\mathbf{k}|\mathbf{v}_\gamma\}\mathcal{G}^\mathbf{k} + \cdots + \{R_q^\mathbf{k}|\mathbf{v}_q\}\mathcal{G}^\mathbf{k}, \quad (\text{A11})$$

where the same one to one correspondence between the coset representative and the arms in the star of \mathbf{k} in (A9) exist.

Appendix B: Application of method of invariant in obtaining TB Hamiltonian

The space group of single layer graphene crystal is 191 (P6/mmm). The point group of the graphene lattice is D_{6h} , The lattice is shown in Fig.1. The carbon atoms are located on the Wyckoff position $\tau = 2c$. We label the two equivalent Wyckoff positions as τ_a and τ_b . The site symmetry group is isomorphic to D_{3h} . The coset representatives in the decomposition in Eq.(A4) are chosen as $R_a^\tau = E$ and $R_b^\tau = I$ for τ_a and τ_b respectively.

Hence the p_z orbitals on these atomic sites form the Γ_4 or Γ_8 irrep of the site symmetry group $\tilde{G}^\tau = D_{3h}$ for single group or double group consideration.

We are concerned with the interaction between orbitals located on the equivalent Wyckoff positions. Since the multiplicity of τ is 2, the site representation $D^\tau(R)$ is a 2×2 matrix and given by

$$D^\tau(R) = \begin{cases} \begin{pmatrix} 1 & 0 \\ 0 & 1 \end{pmatrix} & \text{if } R \in D_{3h} \\ \begin{pmatrix} 0 & 1 \\ 1 & 0 \end{pmatrix} & \text{if } R \notin D_{3h} \end{cases}$$

As $D^\tau(R)$ represents a permutation of the equivalent Wyckoff positions, there is only one unity entry in each row or column with others equal to 0. Let $D^\tau(R)_{\alpha,\beta} = 1$, then the mapping in Eq.(A7) yield

$$R_{\leftarrow}^\tau(R, R_\alpha^\tau) = R_\alpha^{\tau^{-1}} R R_\beta^\tau$$

In this particular case, the mapping is particularly simple and given by

$$R_{\leftarrow}^\tau(R, R_\alpha^\tau) = \begin{cases} R & \text{if } R \in D_{3h} \\ RI & \text{if } R \notin D_{3h} \end{cases}$$

Then the representation matrices

$$D^{\tau,\nu}(R) = D^\tau(R) \otimes D^\nu(R_{\leftarrow}^\tau(R, R_\alpha^\tau)), \quad \forall R \in F.$$

can be constructed. It is important to recognise that the mapping from R to $R_{\leftarrow}^\tau(R, R_\alpha^\tau)$ in the second matrix function is dependent on the row index of $D^\tau(R)$. The same approach is required to construct $D^{\sigma,\mu}(R)$. In this particular case, it is the same as $D^{\tau,\nu}(R)$.

We are now in a position to consider a particular choice of $\mathbf{t}_\ell + \boldsymbol{\sigma}_\alpha$ and $\mathbf{t}'_\ell + \boldsymbol{\tau}_\beta$ in the partition of sum over all Wannier functions. The relevant radial vectors are shown in Fig.11 for the first nearest neighbour (FNN) and second nearest neighbour (SNN) sets.

Onsite interaction: $\mathbf{t}_\ell + \boldsymbol{\sigma}_\alpha = \mathbf{t}'_\ell + \boldsymbol{\tau}_\beta = \boldsymbol{\tau}_a; \boldsymbol{\rho}_1 = \mathbf{0}$.

Hence the phase factor $\exp[i\mathbf{k} \cdot \boldsymbol{\rho}] = 1$. Therefore $D^\rho(R) = 1$. We can then construct the projection operator

$$\mathcal{P}^{\Gamma_1^+} = \frac{1}{|D_{6h}|} \sum_{R \in D_{6h}} D^\rho(R) \otimes D^{\sigma,\mu}(R)^* \otimes D^{\tau,\nu}(R)$$

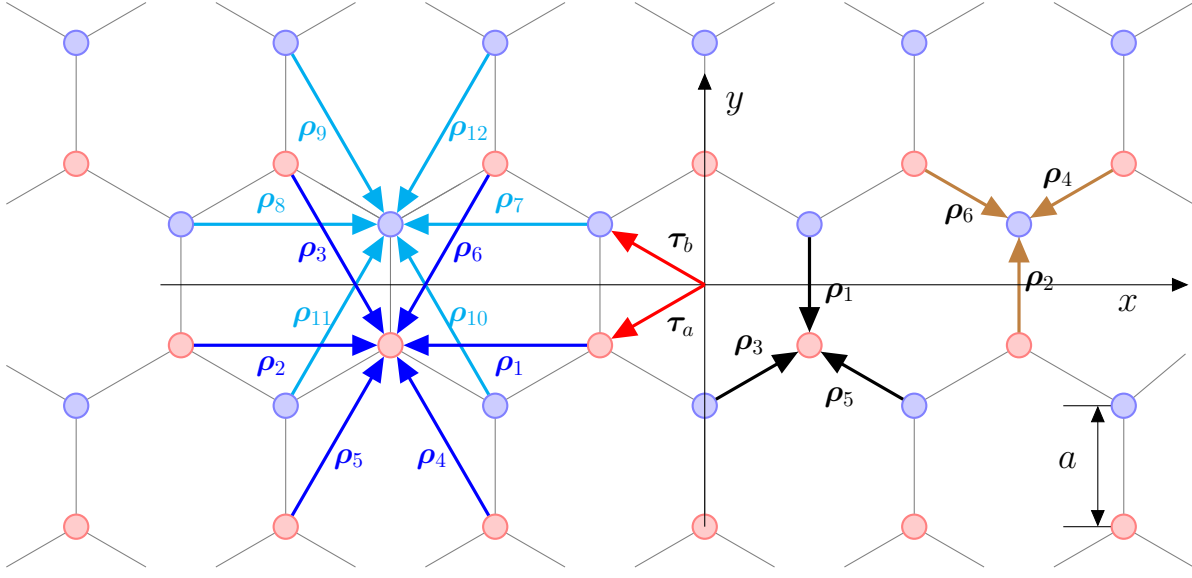


FIG. 11. Distinct radial vectors produced by symmetry operation for first nearest neighbours (black & brown) and second nearest neighbours (blue & cyan).

For single group, setting $\sigma = \tau, \mu = \nu = \Gamma_4$, this yield

$$\mathcal{P}^{\Gamma_4^+} = \frac{1}{2} \begin{pmatrix} 1 & 0 & 0 & 1 \\ 0 & 1 & 1 & 0 \\ 0 & 1 & 1 & 0 \\ 1 & 0 & 0 & 1 \end{pmatrix}$$

Projecting from $[1, 0, 0, 0]^T$ (this correspond to the interaction that specified this shell), we obtain:

$$H = E^\tau \begin{pmatrix} 1 & 0 \\ 0 & 1 \end{pmatrix}$$

where E^τ is the material dependent parameter.

For double group, setting $\sigma = \tau = \tau_a, \mu = \nu = \Gamma_8$, this yield

$$\mathcal{P}^{\Gamma_1^+} = \frac{1}{8} \begin{pmatrix} 1 & 0 & 0 & 0 & 0 & 1 & 0 & 0 & 0 & 0 & 1 & 0 & 0 & 0 & 0 & 1 \\ 0 & 0 & 0 & 0 & 0 & 0 & 0 & 0 & 0 & 0 & 0 & 0 & 0 & 0 & 0 & 0 \\ 0 & 0 & 1 & 0 & 0 & 0 & 0 & 0 & 1 & 1 & 0 & 0 & 0 & 0 & 1 & 0 & 0 \\ 0 & 0 & 0 & 0 & 0 & 0 & 0 & 0 & 0 & 0 & 0 & 0 & 0 & 0 & 0 & 0 & 0 \\ 0 & 0 & 0 & 0 & 0 & 0 & 0 & 0 & 0 & 0 & 0 & 0 & 0 & 0 & 0 & 0 & 0 \\ 1 & 0 & 0 & 0 & 0 & 1 & 0 & 0 & 0 & 0 & 1 & 0 & 0 & 0 & 0 & 1 \\ 0 & 0 & 0 & 0 & 0 & 0 & 0 & 0 & 0 & 0 & 0 & 0 & 0 & 0 & 0 & 0 & 0 \\ 0 & 0 & 1 & 0 & 0 & 0 & 0 & 0 & 1 & 1 & 0 & 0 & 0 & 0 & 1 & 0 & 0 \\ 0 & 0 & 0 & 0 & 0 & 0 & 0 & 0 & 0 & 0 & 0 & 0 & 0 & 0 & 0 & 0 & 0 \\ 0 & 0 & 0 & 0 & 0 & 0 & 0 & 0 & 0 & 0 & 0 & 0 & 0 & 0 & 0 & 0 & 0 \\ 0 & 0 & 0 & 0 & 0 & 0 & 0 & 0 & 0 & 0 & 0 & 0 & 0 & 0 & 0 & 0 & 0 \\ 0 & 0 & 1 & 0 & 0 & 0 & 0 & 0 & 1 & 1 & 0 & 0 & 0 & 0 & 1 & 0 & 0 \\ 0 & 0 & 1 & 0 & 0 & 0 & 0 & 0 & 1 & 1 & 0 & 0 & 0 & 0 & 1 & 0 & 0 \\ 0 & 0 & 0 & 0 & 0 & 0 & 0 & 0 & 0 & 0 & 0 & 0 & 0 & 0 & 0 & 0 & 0 \\ 1 & 0 & 0 & 0 & 0 & 1 & 0 & 0 & 0 & 0 & 1 & 0 & 0 & 0 & 0 & 1 \\ 0 & 0 & 0 & 0 & 0 & 0 & 0 & 0 & 0 & 0 & 0 & 0 & 0 & 0 & 0 & 0 & 0 \\ 0 & 0 & 0 & 0 & 0 & 0 & 0 & 0 & 0 & 0 & 0 & 0 & 0 & 0 & 0 & 0 & 0 \\ 0 & 0 & 1 & 0 & 0 & 0 & 0 & 0 & 1 & 1 & 0 & 0 & 0 & 0 & 1 & 0 & 0 \\ 0 & 0 & 0 & 0 & 0 & 0 & 0 & 0 & 0 & 0 & 0 & 0 & 0 & 0 & 0 & 0 & 0 \\ 0 & 0 & 0 & 0 & 0 & 0 & 0 & 0 & 0 & 0 & 0 & 0 & 0 & 0 & 0 & 0 & 0 \\ 1 & 0 & 0 & 0 & 0 & 1 & 0 & 0 & 0 & 0 & 1 & 0 & 0 & 0 & 0 & 1 \\ 0 & 0 & 0 & 0 & 0 & 0 & 0 & 0 & 0 & 0 & 0 & 0 & 0 & 0 & 0 & 0 & 0 \end{pmatrix}$$

Projecting from $(1, 0, 0, 0, 0, 0, 0, 0, 0, 0, 0, 0, 0, 0, 0, 0)^T$, be obtain

$$H = E^\tau \begin{pmatrix} 1 & 0 & 0 & 0 \\ 0 & 1 & 0 & 0 \\ 0 & 0 & 1 & 0 \\ 0 & 0 & 0 & 1 \end{pmatrix}$$

where E^τ is the material dependent parameter.

Nearest neighbour interaction: $\mathbf{t}_\ell + \sigma_\alpha = \tau_b; \mathbf{t}'_\ell + \tau_\beta = \tau_a; \boldsymbol{\rho}_1 = \tau_a - \tau_b$

The action of the coset representative on $\boldsymbol{\rho}_1$ produces 6 distinct vectors $\boldsymbol{\rho}_1, \dots, \boldsymbol{\rho}_6$ or the corresponding phase factor $\exp[i\mathbf{k} \cdot \boldsymbol{\rho}_r]$. The action of R permutes the 6 vectors or the corresponding phase factor $\exp[i\mathbf{k} \cdot \boldsymbol{\rho}_r]$. Thus the representation matrices $D_{FNN}^\boldsymbol{\rho}(R)$ are 6×6 matrices. We have $D_{FNN}^\boldsymbol{\rho}(E) = \mathbb{1}_{6 \times 6}$. The generators are given by

$$D_{FNN}^\boldsymbol{\rho}(\mathbf{C}_6) = \begin{pmatrix} \mathbf{0} & \sigma_1 & \mathbf{0} \\ \mathbf{0} & \mathbf{0} & \sigma_1 \\ \sigma_1 & \mathbf{0} & \mathbf{0} \end{pmatrix}, \quad D_{FNN}^\boldsymbol{\rho}(\mathbf{I}) = \begin{pmatrix} \sigma_1 & \mathbf{0} & \mathbf{0} \\ \mathbf{0} & \sigma_1 & \mathbf{0} \\ \mathbf{0} & \mathbf{0} & \sigma_1 \end{pmatrix}, \quad D_{FNN}^\boldsymbol{\rho}(\mathbf{C}_2^y) = \begin{pmatrix} \sigma_1 & \mathbf{0} & \mathbf{0} \\ \mathbf{0} & \mathbf{0} & \sigma_1 \\ \mathbf{0} & \sigma_1 & \mathbf{0} \end{pmatrix}.$$

For the rest of the group element of D_{6h} , D^ρ can be constructed from the generators. The projection operator \mathcal{P}^{Γ_1} of dimension 24×24 is constructed. Starting with

The solitary 1 correspond to $\exp\{i\mathbf{k} \cdot \boldsymbol{\rho}_1\}$ and $H(\mathbf{k})_{ba}$ in the term specifying the partition. The following is obtained from projection:

$$\left(\underbrace{0, 0, 1, 0, 0, 0, 1, 0, 0, 0, 0, 1, 0, 0, 1, 0, 0, 0, 1, 0, 0, 1, 0, 0, 1, 0, 0}_{{e^{i\mathbf{k} \cdot \rho_1}}}, \underbrace{0, 1, 0, 0, 0, 0, 1, 0, 0, 0, 0, 1, 0, 0, 0, 1, 0, 0, 0, 1, 0, 0}_{{e^{i\mathbf{k} \cdot \rho_2}}}, \underbrace{0, 0, 1, 0, 0, 0, 0, 1, 0, 0, 0, 0, 1, 0, 0, 0, 0, 1, 0, 0, 0}_{{e^{i\mathbf{k} \cdot \rho_3}}}, \underbrace{0, 0, 0, 1, 0, 0, 0, 0, 1, 0, 0, 0, 0, 1, 0, 0, 0, 0, 1, 0, 0}_{{e^{i\mathbf{k} \cdot \rho_4}}}, \underbrace{0, 0, 0, 0, 1, 0, 0, 0, 0, 1, 0, 0, 0, 0, 1, 0, 0, 0, 1, 0, 0}_{{e^{i\mathbf{k} \cdot \rho_5}}}, \underbrace{0, 0, 0, 0, 0, 1, 0, 0, 0, 0, 1, 0, 0, 0, 0, 1, 0, 0, 0, 1, 0, 0}_{{e^{i\mathbf{k} \cdot \rho_6}}} \right)^T$$

giving rise to a contribution to Hamiltonian from the nearest neighbour partition:

$$H^{FNN} = t_{FNN} \left[\sum_{n=1}^3 \exp(i\mathbf{k} \cdot \boldsymbol{\rho}_{2n-1}) \right] \begin{pmatrix} 0 & 0 \\ 1 & 0 \end{pmatrix} + t_{FNN} \left[\sum_{n=1}^3 \exp(i\mathbf{k} \cdot \boldsymbol{\rho}_{2n}) \right] \begin{pmatrix} 0 & 1 \\ 0 & 0 \end{pmatrix}$$

where t_{FNN} is the material dependent parameter. For double group, the projection operator \mathcal{P}^{Γ_1} is of dimension 96×96 . The contribution to the Hamiltonian from the first nearest neighbour partition is

$$H^{FNN} = t_{FNN} \left[\sum_{n=1}^3 \exp(i\mathbf{k} \cdot \boldsymbol{\rho}_{2n-1}) \right] \begin{pmatrix} \mathbf{0} & \mathbf{0} \\ \sigma_0 & \mathbf{0} \end{pmatrix} + t_{FNN} \left[\sum_{n=1}^3 \exp(i\mathbf{k} \cdot \boldsymbol{\rho}_{2n}) \right] \begin{pmatrix} \mathbf{0} & \sigma_0 \\ \mathbf{0} & \mathbf{0} \end{pmatrix}$$

Second nearest neighbour interaction: $\mathbf{t}_\ell + \boldsymbol{\sigma}_\alpha = \boldsymbol{\tau}_a - \mathbf{a}_1$; $\mathbf{t}'_\ell + \boldsymbol{\tau}_\beta = \boldsymbol{\tau}_a$; $\boldsymbol{\rho}_1 = \boldsymbol{\tau}_a - (\boldsymbol{\tau}_a - \mathbf{a}_1) = \mathbf{a}_1$ There are 12 distinct $\boldsymbol{\rho}$ vectors. Whilst phase term from some of the vectors are numerically the same (e.g. $\boldsymbol{\rho}_1 = \boldsymbol{\rho}_7$), they corresponds to hopping between different sites. The representation matrix for $D_{SNN}^\rho(R)$ are

$$D_{SNN}^{\rho}(C_6) = \sigma_1 \otimes \begin{pmatrix} \mathbf{0} & \sigma_1 & \mathbf{0} \\ \mathbf{0} & \mathbf{0} & \sigma_1 \\ \sigma_1 & \mathbf{0} & \mathbf{0} \end{pmatrix}, \quad D_{SNN}^{\rho}(I) = \sigma_1 \otimes \begin{pmatrix} \sigma_1 & \mathbf{0} & \mathbf{0} \\ \mathbf{0} & \sigma_1 & \mathbf{0} \\ \mathbf{0} & \mathbf{0} & \sigma_1 \end{pmatrix}, \quad D_{SNN}^{\rho}(C_2^y) = \sigma_0 \otimes \begin{pmatrix} \sigma_1 & \mathbf{0} & \mathbf{0} \\ \mathbf{0} & \mathbf{0} & \sigma_1 \\ \mathbf{0} & \sigma_1 & \mathbf{0} \end{pmatrix}.$$

Construct the projection operator \mathcal{P}^{Γ_1} using the same method. Projecting from $(1, 0, 0, 0, \dots)^T$ for single group and making use of the numerical equality between some of the radial vectors, one obtains

$$H^{SNN} = t_{SNN} \left[\sum_{n=1}^6 \exp(i\mathbf{k} \cdot \boldsymbol{\rho}_n) \right] \begin{pmatrix} 1 & 0 \\ 0 & 1 \end{pmatrix}$$

For double group, two linearly independent terms can be projected out from the starting sub-space specified by $\mathbf{t}_\ell + \boldsymbol{\sigma}_\alpha = \boldsymbol{\tau}_a - \mathbf{a}_1$; $\mathbf{t}'_\ell + \boldsymbol{\tau}_\beta = \boldsymbol{\tau}_a$; $\boldsymbol{\rho}_1 = \boldsymbol{\tau}_a - (\boldsymbol{\tau}_a - \mathbf{a}_1) = \mathbf{a}_1$.

Projecting from $(1, 0, 0, 0, 0, 1, 0, 0, \dots)^T$ and $(1, 0, 0, 0, 0, -1, 0, 0, \dots)^T$, the contribution to the Hamiltonian from the second nearest neighbour partition is given by

$$H^{SNN} = t_{SNN} \left[\sum_{n=1}^6 \exp(i\mathbf{k} \cdot \boldsymbol{\rho}_n) \right] \begin{pmatrix} 1 & 0 & 0 & 0 \\ 0 & 1 & 0 & 0 \\ 0 & 0 & 1 & 0 \\ 0 & 0 & 0 & 1 \end{pmatrix} + t'_{SNN} \left[\sum_{n=1}^6 (-1)^{(n-1)} \exp(i\mathbf{k} \cdot \boldsymbol{\rho}_n) \right] \begin{pmatrix} 1 & 0 & 0 & 0 \\ 0 & -1 & 0 & 0 \\ 0 & 0 & -1 & 0 \\ 0 & 0 & 0 & 1 \end{pmatrix}$$

Here t_{SNN} and t'_{SNN} are two distinct material dependent parameters. The existence of the second symmetry permitted term is critical in the topology of the band structure of graphene. See Sec.V for detail.

Appendix C: Information for constructing TB Hamiltonian involving various Wannier functions centred on Wyckoff position 2c.

The bases of the Hamiltonian are band representations (TB bases) derived from the following Wannier functions localised on Wyckoff position 2c. The specific order and phase are obtained using projection operators. The irrep labels refers to that of the site symmetry group (D_{3h}). For simplicity, we define $\epsilon = (1 + i)/2$.

Order of basis: single group

Γ_1	a: Γ_1^s	a:s
	b: Γ_1^s	b:s
Γ_4	a: $\Gamma_4^{p_z}$	a: p_z
	b: $\Gamma_4^{p_z}$	b: p_z
Γ_5	a: $\Gamma_5^{d_{yz,zx}}$: 1	a: d_{yz}
	a: $\Gamma_5^{d_{yz,zx}}$: 2	a: $-d_{zx}$
	b: $\Gamma_5^{d_{yz,zx}}$: 1	b: d_{yz}
	b: $\Gamma_5^{d_{yz,zx}}$: 2	b: $-d_{zx}$
Γ_6	a: $\Gamma_6^{p_{x,y}}$: 1	a: p_x
	a: $\Gamma_6^{p_{x,y}}$: 2	a: p_y
	b: $\Gamma_6^{p_{x,y}}$: 1	b: p_x
	b: $\Gamma_6^{p_{x,y}}$: 2	b: p_y

Order of basis: double group

$\Gamma_7(s)$	a: $\Gamma_7 : 1$	a:s \downarrow	$\Gamma_8(p_z)$	a: $\Gamma_8^{p_z} : 1$	a: $p_z \downarrow$
	a: $\Gamma_7 : 2$	a:s \uparrow		a: $\Gamma_8^{p_z} : 2$	a: $-p_z \uparrow$
	b: $\Gamma_7 : 1$	b:s \downarrow		b: $\Gamma_8^{p_z} : 1$	b: $p_z \downarrow$
	b: $\Gamma_7 : 2$	b:s \uparrow ,		b: $\Gamma_8^{p_z} : 2$	b: $-p_z \uparrow$
$\Gamma_8(p_{x,y})$	a: $\Gamma_8^{p_{x,y}} : 1$	a:($\epsilon p_x \uparrow + \epsilon^* p_y \uparrow$)	$\Gamma_7(d_{yz,zx})$	a: $\Gamma_7^{d_{yz,zx}} : 1$	a:($\epsilon d_{yz} \uparrow - \epsilon^* d_{zx} \uparrow$)
	a: $\Gamma_8^{p_{x,y}} : 2$	a:($\epsilon p_x \downarrow + \epsilon^* p_y \downarrow$)		a: $\Gamma_7^{d_{yz,zx}} : 2$	a:($\epsilon d_{yz} \downarrow + \epsilon^* d_{zx} \downarrow$)
	b: $\Gamma_8^{p_{x,y}} : 1$	b:($\epsilon p_x \uparrow + \epsilon^* p_y \uparrow$)		b: $\Gamma_7^{d_{yz,zx}} : 1$	b:($\epsilon d_{yz} \uparrow - \epsilon^* d_{zx} \uparrow$)
	b: $\Gamma_8^{p_{x,y}} : 2$	b:($\epsilon p_x \downarrow + \epsilon^* p_y \downarrow$)		b: $\Gamma_7^{d_{yz,zx}} : 2$	b:($\epsilon d_{yz} \downarrow + \epsilon^* d_{zx} \downarrow$)
$\Gamma_9(p_{x,y})$	a: $\Gamma_9^{p_{x,y}} : 1$	a:($\epsilon^* p_x \uparrow + \epsilon p_y \uparrow$)	$\Gamma_9(d_{yz,zx})$	a: $\Gamma_9^{d_{yz,zx}} : 1$	a:($\epsilon d_{yz} \downarrow - \epsilon^* d_{zx} \downarrow$)
	a: $\Gamma_9^{p_{x,y}} : 2$	a:($\epsilon^* p_x \downarrow - \epsilon p_y \downarrow$)		a: $\Gamma_9^{d_{yz,zx}} : 2$	a:($-\epsilon d_{yz} x \uparrow + \epsilon^* d_{zx} \uparrow$)
	b: $\Gamma_9^{p_{x,y}} : 1$	b:($\epsilon^* p_x \uparrow + \epsilon p_y \uparrow$)		b: $\Gamma_9^{d_{yz,zx}} : 1$	b:($\epsilon d_{yz} \downarrow - \epsilon^* d_{zx} \downarrow$)
	b: $\Gamma_9^{p_{x,y}} : 2$	b:($\epsilon^* p_x \downarrow - \epsilon p_y \downarrow$)		b: $\Gamma_9^{d_{yz,zx}} : 2$	b:($-\epsilon d_{yz} x \uparrow + \epsilon^* d_{zx} \uparrow$)

Graphene generators matrices

The matrix representations of the Hamiltonian between the above basis is constructed, for successive radial shells, from 1) material dependent parameters, 2) exponential phase factors $\exp(i\mathbf{k} \cdot \boldsymbol{\rho}_n)$, and 3) generator matrices associated with the symmetry of the bases for the given $\boldsymbol{\rho}_n$. Reading from the generator matrices listed below, the matrix representation of Hamiltonian between the Γ_7^s and $\Gamma_8^{p_{x,y}}$ is obtained as

$$H_{\Gamma_7^s, \Gamma_8^{p_{x,y}}} = H_{\Gamma_7^s, \Gamma_8^{p_{x,y}}}^{ZNN} (\equiv 0) + H_{\Gamma_7^s, \Gamma_8^{p_{x,y}}}^{FNN} + H_{\Gamma_7^s, \Gamma_8^{p_{x,y}}}^{SNN} + \dots$$

The contributing terms are:

$$H_{\Gamma_7^s, \Gamma_8^p}^{FNN} = t_{\Gamma_7^s, \Gamma_8^p}^{FNN} \left\{ e^{ik \cdot \rho_1} \begin{pmatrix} 0 & 0 & 0 & 0 \\ 0 & 0 & 0 & 0 \\ 0 & -1 & 0 & 0 \\ 1 & 0 & 0 & 0 \end{pmatrix} + e^{ik \cdot \rho_2} \begin{pmatrix} 0 & 0 & 0 & -1 \\ 0 & 0 & 1 & 0 \\ 0 & 0 & 0 & 0 \\ 0 & 0 & 0 & 0 \end{pmatrix} \right. \\ \left. + e^{ik \cdot \rho_3} \begin{pmatrix} 0 & 0 & 0 & 0 \\ 0 & 0 & 0 & 0 \\ 0 & \omega^* & 0 & 0 \\ -\omega & 0 & 0 & 0 \end{pmatrix} + e^{ik \cdot \rho_4} \begin{pmatrix} 0 & 0 & 0 & \omega^* \\ 0 & 0 & -\omega & 0 \\ 0 & 0 & 0 & 0 \\ 0 & 0 & 0 & 0 \end{pmatrix} \right. \\ \left. + e^{ik \cdot \rho_5} \begin{pmatrix} 0 & 0 & 0 & 0 \\ 0 & 0 & 0 & 0 \\ 0 & \omega & 0 & 0 \\ -\omega^* & 0 & 0 & 0 \end{pmatrix} + e^{ik \cdot \rho_6} \begin{pmatrix} 0 & 0 & 0 & \omega \\ 0 & 0 & -\omega^* & 0 \\ 0 & 0 & 0 & 0 \\ 0 & 0 & 0 & 0 \end{pmatrix} \right\}.$$

$$H_{\Gamma_7^s, \Gamma_8^p}^{SNN} = t_{\Gamma_7^s, \Gamma_8^p}^{SNN:A} \left\{ (e^{ik \cdot \rho_1} - e^{ik \cdot \rho_2}) \begin{pmatrix} 0 & 1 & 0 & 0 \\ 1 & 0 & 0 & 0 \\ 0 & 0 & 0 & -1 \\ 0 & 0 & -1 & 0 \end{pmatrix} + (e^{ik \cdot \rho_3} - e^{ik \cdot \rho_4}) \begin{pmatrix} 0 & -\epsilon^* & 0 & 0 \\ -\epsilon & 0 & 0 & 0 \\ 0 & 0 & 0 & \epsilon^* \\ 0 & 0 & \epsilon & 0 \end{pmatrix} \right. \\ \left. + (e^{ik \cdot \rho_5} - e^{ik \cdot \rho_6}) \begin{pmatrix} 0 & -\epsilon & 0 & 0 \\ -\epsilon^* & 0 & 0 & 0 \\ 0 & 0 & 0 & \epsilon \\ 0 & 0 & \epsilon^* & 0 \end{pmatrix} \right\} + t_{\Gamma_7^s, \Gamma_8^p}^{SNN:B} \left\{ (e^{ik \cdot \rho_1} + e^{ik \cdot \rho_2}) \begin{pmatrix} 0 & -1 & 0 & 0 \\ 1 & 0 & 0 & 0 \\ 0 & 0 & 0 & -1 \\ 0 & 0 & 1 & 0 \end{pmatrix} \right. \\ \left. + (e^{ik \cdot \rho_3} + e^{ik \cdot \rho_4}) \begin{pmatrix} 0 & \epsilon^* & 0 & 0 \\ -\epsilon & 0 & 0 & 0 \\ 0 & 0 & 0 & \epsilon^* \\ 0 & 0 & -\epsilon & 0 \end{pmatrix} + (e^{ik \cdot \rho_5} + e^{ik \cdot \rho_6}) \begin{pmatrix} 0 & \epsilon & 0 & 0 \\ -\epsilon^* & 0 & 0 & 0 \\ 0 & 0 & 0 & \epsilon \\ 0 & 0 & -\epsilon^* & 0 \end{pmatrix} \right\}$$

The material dependent parameters (up to first nearest neighbour interaction) can be related to the SK parameter (ignoring the normalising overlap integral) as the follows:

$$\begin{array}{llllllll} t_{\Gamma_1^s, \Gamma_1^s}^{ZNN} & t_{\Gamma_4^p, \Gamma_4^p}^{ZNN} & t_{\Gamma_6^p, y, \Gamma_6^p}^{ZNN} & t_{\Gamma_1^s, \Gamma_1^s}^{FNN} & t_{\Gamma_4^p, \Gamma_4^p}^{FNN} & t_{\Gamma_1^s, \Gamma_6^p}^{FNN} & t_{\Gamma_6^p, y, \Gamma_6^p}^{FNN:A} & t_{\Gamma_6^p, y, \Gamma_6^p}^{FNN:B} \\ \epsilon_s & \epsilon_p & \epsilon_p & V_{ss\sigma} & V_{pp\pi} & V_{sp\sigma} & (V_{pp\sigma} + V_{pp\pi})/2 & (V_{pp\pi} - V_{pp\sigma})/2 \end{array}$$

The subscript to the generator matrices listed in the table below indicated the exponential function associated with the matrix. For example, A_{1-2} would correspond to

$$[\exp(i\mathbf{k} \cdot \rho_1) - \exp(i\mathbf{k} \cdot \rho_2)] A.$$

On-site (ZNN): These are simply identity matrices with relevant dimensions.

First nearest neighbour (FNN): $\omega = (1 + \sqrt{3})/2$.

$\Gamma_1 : \Gamma_1$	$\begin{pmatrix} 0 & 0 \\ 1 & 0 \end{pmatrix}_{1+3+5} \begin{pmatrix} 0 & 1 \\ 0 & 0 \end{pmatrix}_{2+4+6}$
$\Gamma_4 : \Gamma_4$	$\begin{pmatrix} 0 & 0 & 0 & 0 \\ 0 & 2 & 0 & 0 \\ 0 & 0 & -\sqrt{3} & -1 \\ 0 & 0 & 0 & 0 \end{pmatrix}_4 \begin{pmatrix} 0 & 0 & 0 & 2 \\ 0 & 0 & 0 & 0 \\ 0 & 0 & 0 & 0 \\ \sqrt{3} & -1 & 0 & 0 \end{pmatrix}_5 \begin{pmatrix} 0 & 0 & 0 & 0 \\ -\sqrt{3} & -1 & 0 & 0 \\ 0 & 0 & \sqrt{3} & -1 \\ 0 & 0 & 0 & 0 \end{pmatrix}_6$
$\Gamma_1 : \Gamma_6$ $(\frac{1}{2} \times)$	$\begin{pmatrix} 0 & 0 & 0 & 0 \\ 0 & 0 & 0 & 0 \\ 0 & 0 & 0 & 0 \\ 0 & 0 & 0 & 0 \end{pmatrix}_1 \begin{pmatrix} 0 & 0 & 2 & 0 \\ 0 & 0 & 0 & 0 \\ 0 & 0 & 0 & 0 \\ \sqrt{3} & -1 & 0 & 0 \end{pmatrix}_2 \begin{pmatrix} 0 & 0 & 0 & 0 \\ -\sqrt{3} & -1 & 0 & 0 \\ 0 & 0 & \sqrt{3} & -1 \\ 0 & 0 & 0 & 0 \end{pmatrix}_3$
$\Gamma_4 : \Gamma_5$ $(\frac{1}{2} \times)$	$\begin{pmatrix} 0 & 0 & 0 & 0 \\ 2 & 0 & 0 & 0 \\ 0 & 0 & -1 & \sqrt{3} \\ 0 & 0 & 0 & 0 \end{pmatrix}_4 \begin{pmatrix} 0 & 0 & 2 & 0 \\ 0 & 0 & 0 & 0 \\ 0 & 0 & 0 & 0 \\ -1 & -\sqrt{3} & 0 & 0 \end{pmatrix}_5 \begin{pmatrix} 0 & 0 & 0 & 0 \\ -1 & \sqrt{3} & 0 & 0 \\ 0 & 0 & -1 & -\sqrt{3} \\ 0 & 0 & 0 & 0 \end{pmatrix}_6$
$\Gamma_5 : \Gamma_5 : A$	$\begin{pmatrix} 0 & 0 & 0 & 0 \\ 0 & 0 & 0 & 0 \\ 1 & 0 & 0 & 0 \\ 0 & 1 & 0 & 0 \end{pmatrix}_{1+3+5} \begin{pmatrix} 0 & 0 & 1 & 0 \\ 0 & 0 & 0 & 1 \\ 0 & 0 & 0 & 0 \\ 0 & 0 & 0 & 0 \end{pmatrix}_{2+4+6}$
$\Gamma_6 : \Gamma_6 : A$	$\begin{pmatrix} 0 & 0 & 0 & 0 \\ 0 & 0 & 0 & 0 \\ 0 & 0 & 0 & 0 \\ 0 & 0 & 0 & 0 \end{pmatrix}_{1+3+5} \begin{pmatrix} 0 & 0 & 1 & 0 \\ 0 & 0 & 0 & 1 \\ 0 & 0 & 0 & 0 \\ 0 & 0 & 0 & 0 \end{pmatrix}_{2+4+6}$
$\Gamma_5 : \Gamma_5 : B$ $\Gamma_6 : \Gamma_6 : B$ $(\frac{1}{2} \times)$	$\begin{pmatrix} 0 & 0 & 0 & 0 \\ 0 & 0 & 0 & 0 \\ 2 & 0 & 0 & 0 \\ 0 & -2 & 0 & 0 \end{pmatrix}_1 \begin{pmatrix} 0 & 0 & 2 & 0 \\ 0 & 0 & 0 & -2 \\ 0 & 0 & 0 & 0 \\ 0 & 0 & 0 & 0 \end{pmatrix}_2 \begin{pmatrix} 0 & 0 & 0 & 0 \\ 0 & 0 & -\sqrt{3} & 0 & 0 \\ -\sqrt{3} & 1 & 0 & 0 \\ 0 & 0 & 0 & 0 \end{pmatrix}_3$ $\begin{pmatrix} 0 & 0 & -1 & -\sqrt{3} \\ 0 & 0 & -\sqrt{3} & 1 \\ 0 & 0 & 0 & 0 \\ 0 & 0 & 0 & 0 \end{pmatrix}_4 \begin{pmatrix} 0 & 0 & 0 & 0 \\ 0 & 0 & 0 & 0 \\ -1 & \sqrt{3} & 0 & 0 \\ \sqrt{3} & 1 & 0 & 0 \end{pmatrix}_5 \begin{pmatrix} 0 & 0 & -1 & \sqrt{3} \\ 0 & 0 & \sqrt{3} & 1 \\ 0 & 0 & 0 & 0 \\ 0 & 0 & 0 & 0 \end{pmatrix}_6$

Second Nearest Neighbour (SNN): $\omega = (1 + \sqrt{3})/2$.

$\Gamma_1 : \Gamma_1$	$\begin{pmatrix} 1 & 0 \\ 0 & 1 \end{pmatrix}_{1+...+6}$
$\Gamma_4 : \Gamma_4$	$\begin{pmatrix} 2 & 0 & 0 & 0 \\ 0 & 0 & -2 & 0 \end{pmatrix}_{1-2}, \begin{pmatrix} -1 & \sqrt{3} & 0 & 0 \\ 0 & 0 & 1 & -\sqrt{3} \end{pmatrix}_{3-4}, \begin{pmatrix} -1 & -\sqrt{3} & 0 & 0 \\ 0 & 0 & 1 & \sqrt{3} \end{pmatrix}_{5-6}$
$\Gamma_1 : \Gamma_6 : A$ $(\frac{1}{2} \times)$	$\begin{pmatrix} 0 & 2 & 0 & 0 \\ 0 & 0 & 0 & 2 \end{pmatrix}_{1+2}, \begin{pmatrix} -\sqrt{3} & -1 & 0 & 0 \\ 0 & 0 & -\sqrt{3} & -1 \end{pmatrix}_{3+4}, \begin{pmatrix} \sqrt{3} & -1 & 0 & 0 \\ 0 & 0 & \sqrt{3} & -1 \end{pmatrix}_{5+6}$
$\Gamma_4 : \Gamma_5 : A$ $(\frac{1}{2} \times)$	$\begin{pmatrix} 2 & 0 & 0 & 0 \\ 0 & 0 & 2 & 0 \end{pmatrix}_{1+2}, \begin{pmatrix} -1 & \sqrt{3} & 0 & 0 \\ 0 & 0 & -1 & \sqrt{3} \end{pmatrix}_{3+4}, \begin{pmatrix} -1 & -\sqrt{3} & 0 & 0 \\ 0 & 0 & -1 & -\sqrt{3} \end{pmatrix}_{5+6}$
$\Gamma_4 : \Gamma_5 : B$ $(\frac{1}{2} \times)$	$\begin{pmatrix} 0 & 2 & 0 & 0 \\ 0 & 0 & 0 & -2 \end{pmatrix}_{1-2}, \begin{pmatrix} -\sqrt{3} & -1 & 0 & 0 \\ 0 & 0 & \sqrt{3} & 1 \end{pmatrix}_{3-4}, \begin{pmatrix} \sqrt{3} & -1 & 0 & 0 \\ 0 & 0 & -\sqrt{3} & 1 \end{pmatrix}_{5-6}$
$\Gamma_5 : \Gamma_5 : A$	$\begin{pmatrix} 1 & 0 & 0 & 0 \\ 0 & 1 & 0 & 0 \end{pmatrix}$
$\Gamma_6 : \Gamma_6 : A$	$\begin{pmatrix} 0 & 0 & 1 & 0 \\ 0 & 0 & 0 & 1 \end{pmatrix}_{1+...+6}$
$\Gamma_5 : \Gamma_5 : B$	$\begin{pmatrix} 2 & 0 & 0 & 0 \\ 0 & -2 & 0 & 0 \end{pmatrix}_{1+2} \begin{pmatrix} -1 & -\sqrt{3} & 0 & 0 \\ -\sqrt{3} & 1 & 0 & 0 \end{pmatrix}_{3+4} \begin{pmatrix} -1 & \sqrt{3} & 0 & 0 \\ \sqrt{3} & 1 & 0 & 0 \end{pmatrix}_{5+6}$
$\Gamma_6 : \Gamma_6 : B$ $(\frac{1}{2} \times)$	$\begin{pmatrix} 0 & 0 & 2 & 0 \\ 0 & 0 & 0 & -2 \end{pmatrix}_{1+2} \begin{pmatrix} 0 & 0 & -1 & -\sqrt{3} \\ 0 & 0 & -\sqrt{3} & 1 \end{pmatrix}_{3+4} \begin{pmatrix} 0 & 0 & -1 & \sqrt{3} \\ 0 & 0 & \sqrt{3} & 1 \end{pmatrix}_{5+6}$
$\Gamma_5 : \Gamma_5 : C$	$\begin{pmatrix} 0 & 2 & 0 & 0 \\ 2 & 0 & 0 & 0 \end{pmatrix} \begin{pmatrix} \sqrt{3} & -1 & 0 & 0 \\ -1 & -\sqrt{3} & 0 & 0 \end{pmatrix}_{3-4} \begin{pmatrix} -\sqrt{3} & -1 & 0 & 0 \\ -1 & \sqrt{3} & 0 & 0 \end{pmatrix}_{5-6}$
$\Gamma_6 : \Gamma_6 : C$ $(\frac{1}{2} \times)$	$\begin{pmatrix} 0 & 0 & 0 & -2 \\ 0 & 0 & -2 & 0 \end{pmatrix}_{1-2} \begin{pmatrix} 0 & 0 & -\sqrt{3} & 1 \\ 0 & 0 & 1 & \sqrt{3} \end{pmatrix}_{3-4} \begin{pmatrix} 0 & 0 & \sqrt{3} & 1 \\ 0 & 0 & 1 & -\sqrt{3} \end{pmatrix}_{5-6}$
$\Gamma_5 : \Gamma_5 : D$	$\begin{pmatrix} 0 & 1 & 0 & 0 \\ -1 & 0 & 0 & 0 \end{pmatrix}$
$\Gamma_6 : \Gamma_6 : D$	$\begin{pmatrix} 0 & 0 & 0 & -1 \\ 0 & 0 & 1 & 0 \end{pmatrix}_{1-2+3-4+5-6}$

¹ J. Zak, **Phys. Rev. B**, **23**, 2824 (1981).

² J. Zak, **Phys. Rev. B**, **26**, 3010 (1982).

³ Barry Bradlyn, L. Elcoro, Jeniffer Cano, M.G. Vergniory, Zhijun Wang, C. Felser, M.I. Aroyo, and B. Andrei Bernevig, **Nature**, **547**, 298 (2017).

⁴ Feng Tang, Hoi Chun Po, Ashvin Vishwanath, and Xianggang Wan, **Nature Phys.** **15**, 470 (2019).

⁵ Hoi Chun Po, Ashvin Vishwanath, and Haruki Watanabi, **Nature Comm.** **8**, 50, (2017)

⁶ Hoi Chun Po, **J. Phys: Cond. Mat.** **32**, 263001 (2020).

⁷ Jennifer Cano, Barry Bradlyn, Zhijun Wang, L. Elcoro, M.G. Vergniory, C. Felser, M.I. Aroyo, and B. Andrei Bernevig, **Phys. Rev. B** **97**, 035139 (2018)

⁸ Jennifer Cano and Barry Bradlyn, **Ann. Rev. Cond. Mat. Phys.** **12**, 225 (2021)

⁹ M G Vergniory, L Elcoro, Zhijun Wang, Jennifer Cano, C Felser, M I Aroyo, B Andrei Bernevig, and Barry Bradlyn, **Phys. Rev. E** **96**, 023310 (2017)

¹⁰ R. A. Evarestov, and V. P. Smirnov, *phys. stat. sol. (b)*, **122**, 231 (1984); *ibid* 529 (1984).

¹¹ Luis Elcoro, Barry Bradlyn, Zhijun Wang, Maia G. Vergniory, Jennifer Cano, Claudia Felser, B. Andrei Bernevig, Danel Orobengoa, Gemma de la Flora and Mois I. Aroyo, **J. Appl. Cryst.**, **50**, 1457 (2017)

¹² “Symmetry, Invariants, Topology”, Editor L. Michel, **Physics Reports**, **341** (2001)

¹³ J. Zak, **Phys. Rev. B**, **25**, 1344 (1982).

¹⁴ Henri Bacry, **Commun. Math. Phys.** **153**, 359, (1993).

¹⁵ The original work of Zak[1], Evarestov[10] and more recent literature[4,7] appears to define the band representation without explicit reference to the Wyckoff position in the “centre” of the Wannier function. See for example Eq.(4) of Ref.[7] or Eq.(3a) of Ref[10]

$$a_{i,\alpha}(\mathbf{k}, \mathbf{r}) = \sum_{\mu} \exp \{i \mathbf{k} \cdot \mathbf{t}_{\mu}\} W_{i,\alpha}(\mathbf{r} - \mathbf{t}_{\mu}).$$

If one takes these definition literally, the Wannier function is localised at the chosen origin of the unit cell instead of \mathbf{q}_{α} . However, from text before Eq.4, Eq.4 and Eq.7a of Ref.[10], implicit in these definition is that $W_{i,\alpha}(\mathbf{r} - \mathbf{t}_{\mu}) \equiv W_{i,\alpha}(\mathbf{r} - \mathbf{t}_{\mu} - \mathbf{q}_{\alpha})$. If one follows through with the

argument, $\mathbf{t}_{\alpha\beta}$ may not be a lattice vector and additional phase term in Eq.9 appears. Thus transformation matrices in the literature is not correct, particularly at HSPs on the surface of BZ. In Ref.[4], the TB basis (Eq.33, supplement) is used, but appropriate phase term (Γ_{gauge} in Eq.(13) of this manuscript) is missing in the transformation properties(Eq.37 supplement). It did not recognise that $R\mathbf{k} - \mathbf{k} = \mathbf{g}_R \neq \mathbf{0}$ can occur even under the action of $\mathcal{G}^{\mathbf{k}}$. The character obtained from Eq.37(supplement) does not have explicit Wyckoff position dependence at HSPs.

- ¹⁶ J.C. Slater, and G. Koster, **Phys. Rev.** **94**, 1498, (1954).
- ¹⁷ EBR are band representations induced from Wyckoff position whose site symmetry group is maximal. It can not be decomposed into other EBRs. See 19 chapter VI. Bands represented by an EBR is connected.
- ¹⁸ PEBR is EBR which obeys time reversal symmetry in addition to those afforded by the space group.
- ¹⁹ L. Michel and J. Zak, **Physics Reports**, **341**, 377 (2001).
- ²⁰ Hoi Chun Po, Haruki Watanabi, and Ashvin Vishwanath, **Phys. Rev. Lett.** **121**, 126402 (2018).
- ²¹ Jennifer Cano, Barry Bradlyn, Zhijun Wang, L. Elcoro, M.G. Verniory, C. Felser, M.I. Aroyo, and B. Andrei Bernevig, **Phys. Rev. Lett** **120**, 266401 (2018)
- ²² C.J. Bradley, and A.P. Cracknell, “The Mathematical Theory of Symmetry in Solid”, Oxford University Press, 2010.
- ²³ For example, BANDREP from [11] reports the decomposition of BR induced from p_z orbital (A'') on Wyckoff position 2c yield $\Gamma_2^- \oplus \Gamma_3^+$, $M_2^- \oplus M_3^+$, K_6 . A primary reason of the difference from the present work is the choice of real space configuration in BANDREP differing (90° rotation about z axis) from those in Ref.[28 and 29]. Even with these changes in real space configuration, the decomposition should be $\Gamma_2^- \oplus \Gamma_3^+$, $M_2^- \oplus M_3^+$, K_5 . The assignment of K_6 instead of K_5 could not be explained.
- ²⁴ L.P. Bouckaert, R. Smoluchowski, and E.P. Wigner, **Phys. Rev.** **50**, 58 (1936).
- ²⁵ The author thanks Prof. Bradlyn for assisting in finding the relevant parameters.
- ²⁶ Sergej Konschuh, Martin Gmitra, and Jaroslav Fabian, **Phys. Rev. B**, **82**, 245412 (2010).
- ²⁷ Warren J. Elder, Eng Soon Tok, Dimitri D Vvedensky, and Jing Zhang, <https://arxiv.org/abs/1306.2520>
- ²⁸ “International Table for Crystallography” Vol A., Kluwer Academic Press, 2005.

²⁹ “International Table for Crystallography” Vol E., Kluwer Academic Press, 2002.

³⁰ George F. Koster, John D. Dimmock, Robert G. Wheeler and Hermann Statz, “Properties of the thirty-two point groups” MIT Press (1963)